AAPM TG 241: MRI-guided Focused Ultrasound

Allison Payne
Department of Radiology and Imaging Sciences, University of Utah, Salt Lake City, UT 84112, USA

Rajiv Chopra
Department of Radiology, UT Southwestern Medical Center, Dallas, TX 75390, USA

Nicolas Ellens
Acetara Acoustic Laboratories, Longmont, CO 80501, USA

Lili Chen
Department of Radiation Oncology, Fox Chase Cancer Center, Philadelphia, PA 19111, USA

Pejman Ghanouni
Department of Radiology, Stanford University, Stanford, CA 94305, USA

Steffen Sammet
Department of Radiology, University of Chicago, Chicago, IL 60637, USA

Chris Diederich
Department of Radiation Oncology, University of California San Francisco, San Francisco, CA 94115, USA

Gail ter Haar
The Institute of Cancer Research, London SW7 3RP, England

Dennis Parker
Department of Radiology and Imaging Sciences, University of Utah, Salt Lake City, UT 84112, USA

Chrit Moonen
Imaging Division, University Medical Center Utrecht, 3508 GA, Utrecht, the Netherlands

Jason Stafford
Department of Imaging Physics, MD Anderson Cancer Center, Houston, TX 77054, USA

Eduardo Moros
Department of Radiation Oncology, Moffitt Cancer Center, Tampa, FL 33612, USA

David Schlesinger
Department of Radiation Oncology, University of Virginia, Charlottesville, VA 22908, USA

Stanley Benedict
Department of Radiation Oncology, UC Davis, Sacramento, CA 95817, USA

Keith Wear
U.S. Food and Drug Administration, Silver Spring, MD 20993, USA

Ari Partanen

Profound Medical, Inc., Mississauga, ON, Canada

Keyvan Farahani
National Cancer Institute, National Institutes of Health, Rockville, MD 20852, USA

Disclosure Statement

The Chair of Task Group-241: MRI- Guided Focused Ultrasound has reviewed the required Conflict of Interest statement of file for each member of Task Group-241: MRI-Guided Focused Ultrasound and determined that disclosure of potential Conflicts of Interest is an adequate management plan. Disclosures of potential Conflict of Interest for each member of Task Group-241: MRI- Guided Focused Ultrasound are found at the close of this document.

Table of Contents

Acronym List

ADC	Apparent Diffusion Coefficient
CDRH	Center for Devices and Radiological Health
CE-MRI	Contrast-Enhanced Magnetic Resonance Imaging
CEM	Cumulative Equivalent Minutes
DCE	Dynamic Contrast Enhanced
DQA	Daily Quality Assurance
FDA	Food and Drug Administration
GUI	Graphical User Interface
HIFU	High Intensity Focused Ultrasound
IDE	Investigational Device Exemption
MRgFUS	Magnetic Resonance-guided Focused Ultrasound
MRTI	Magnetic Resonance Temperature Imaging
MRI	Magnetic Resonance Imaging
NPV	Non-Perfused Volume
PRF	Proton Resonance Frequency
QA	Quality Assurance
RF	Radiofrequency
ROI	Region of Interest
SNR	Signal to Noise Ratio
TDV	Thermal Dose Volume
TMM	Tissue Mimicking Materials
T1w/T2w	T1-weighted/T2-weighted MRI images

Abstract:

This report prepared by the American Association of Physicist in Medicine (AAPM) Task Group 241 addresses the issues of interest to the medical physics community, specific to the body MRgFUS system configuration, and provides recommendations on how to successfully implement and maintain a clinical MRgFUS program. The following sections describe the key features of typical MRgFUS systems and clinical workflow. Commonly used terms, metrics and physics are defined and sources of uncertainty that affect MRgFUS procedures are described. Finally, safety and quality assurance procedures are explained, the recommended role of the medical physicist in MRgFUS procedures is described, and regulatory requirements for planning clinical trials are detailed. This report is limited in scope to clinical body MRgFUS systems approved or currently undergoing clinical trials in the United States.

Keywords:

Magnetic resonance imaging, Focused ultrasound, HIFU

1. Introduction

Magnetic resonance image-guided focused ultrasound, commonly referred to as MRgFUS or MRgHIFU, is a non-ionizing image-guided interventional technology that couples the energy delivery capabilities of therapeutic focused ultrasound with magnetic resonance imaging. Unlike other commonly used image-guided minimally invasive interventional therapies such as radiofrequency-, microwave-, laser- or cryo-ablation, MRgFUS is completely non-invasive, potentially resulting in shorter recovery times and reduced infection risks. The utilization of focused ultrasound under MRI guidance allows for accurate delineation of the treatment target, real-time treatment feedback with thermometry maps or other parametric MR images and post-treatment assessment (1). These features have spawned significant clinical interest in MRgFUS, primarily in treatment of solid tumors.

While therapeutic ultrasound is not a new technology, with its use first being reported over 70 years ago (2-4), it was not until coupling the technology with MRI (5,6), to provide non-invasive monitoring of treatments and design and production of clinical body systems that regulatory approval was obtained in 2004 from the US Food and Drug Administration (FDA), initially for thermal ablation treatment of uterine fibroids by a commercial system (7). Further technological advances have led to development of specialized MRgFUS system configurations, such as brain (8) and interstitial probes (9,10). Subsequently, FDA approvals and clearances have been issued for other oncologic and neurologic indications including essential tremor, bone metastases and prostate tissue. In addition, many other clinical indications are at different levels of development with several in clinical trials (11).

The MRgFUS technology is complex and multi-faceted, requiring careful treatment planning, dosimetry and calibration, as well as routine quality assurance and maintenance procedures. MRgFUS procedures often include patient-specific challenges that benefit from input provided by a qualified and experienced physicist well-versed in both MRI and focused ultrasound technologies. For example, known MRgFUS issues and measurement uncertainties that can impede successful procedures may include relatively long treatment times, motion in or around the treatment region, the presence of anatomic structures that cause severe absorption, refraction or reflection of the ultrasound beam, and the protection of proximal critical structures. Therefore, medical physicists can play a critical role in all phases of the MRgFUS development and applications including the identification, management and mitigation of measurement uncertainty sources.

2. Components of a clinical body MRgFUS system

In clinical body MRgFUS systems, the MRI and focused ultrasound components are integrated. The ultrasound transducer can be embedded in the MR imaging table to allow simultaneous imaging and therapy. Although specialized MRI systems are not required, there are specific site and room requirements, most of which were identified in early development of the technology in the 1990's (12,13). Generally ultrasound transmission in the bore of the magnet can proceed simultaneously with imaging since the operating frequency of most body MRgFUS devices is approximately 1 MHz, and the receive bandwidth of the MRI is approximately 64 MHz for 1.5 T MRI systems, increasing with higher field strengths. As shown in the schematic in **Figure 1**, the major components of the clinical MR system include the patient table assembly with an integrated HIFU transducer, a mechanical or electromechanical positioning system to steer and aim the FUS beam into a patient target, RF electronics capable of driving the ultrasound transducer to produce a focused acoustic beam, cooling systems for both the transducer and patient skin interface, and treatment planning and delivery software to enable identification of

treatment targets and monitoring of FUS delivery using real-time MRI thermometry. These components are discussed individually below.

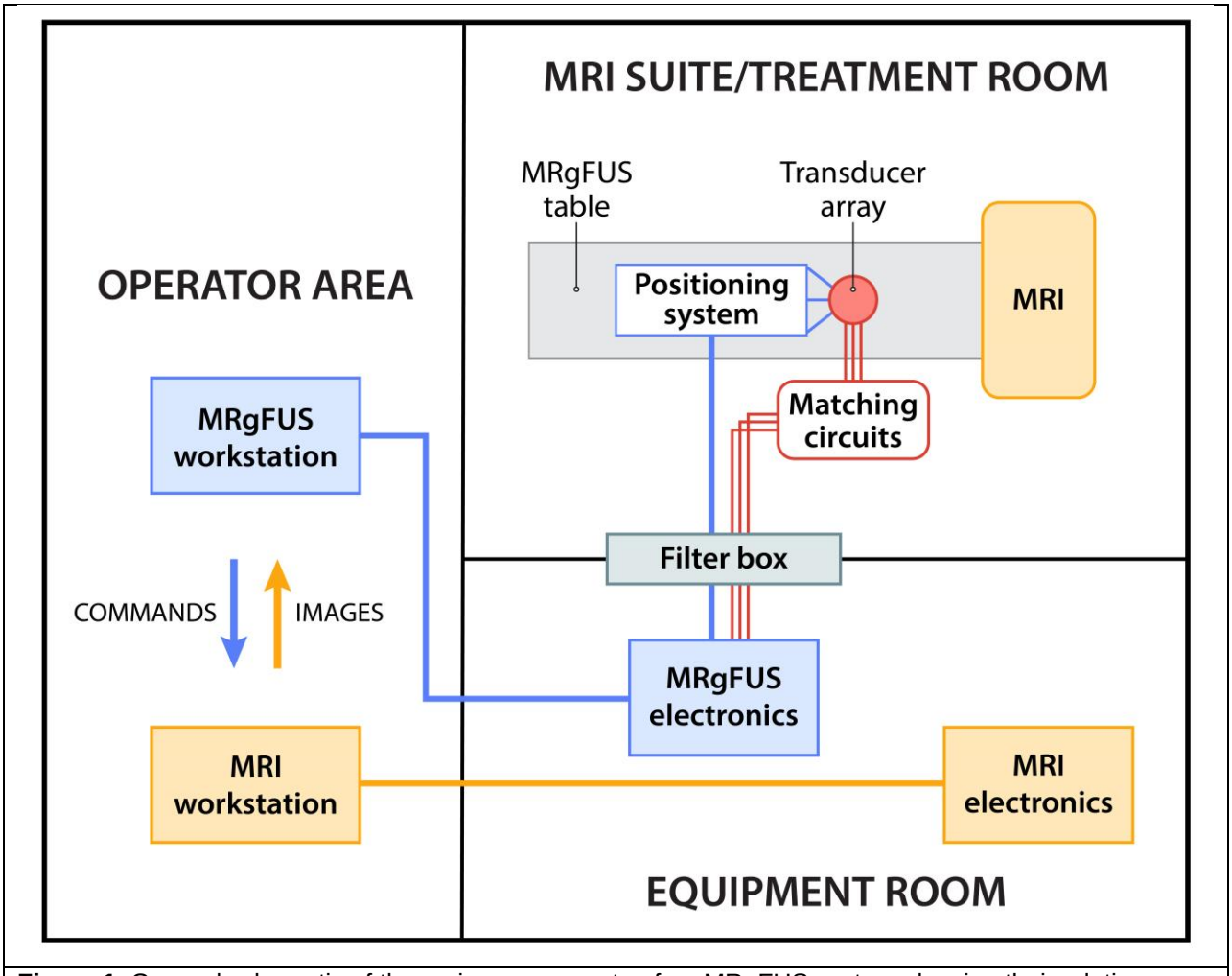

Figure 1: General schematic of the major components of an MRgFUS system showing their relative position to the MRI suite/treatment room, operator area and equipment room.

2.1 MR scanner & supporting infrastructure

At the time of publication, the ExAblate 2000/2100 from Insightec (Insightec Inc., Haifa, Israel) and the Sonalleve system (Profound Medical Corp., Mississauga, ON) are the two body MRgFUS systems used clinically in the United States (14,15). MRgFUS therapy systems can be integrated into conventional clinical 1.5T and 3T MRI systems, with minor modifications to the room and hardware. Often, a more important criterion than field strength is the MRI bore size, with wide bore systems being more amenable to interventional procedures such as MRgFUS. The Faraday shield on the MRI suite typically requires installation of a grounded RF panel for transmission of the electrical signals from the focused ultrasound generators located in the equipment room. Electrical signals are filtered to prevent the transmission of interference frequencies into the MRI suite. Waveguides may also be required to pass fluids for the cooling circuits from the equipment room to the MRgFUS system. The installation of these panels typically requires minor construction and can be done on an existing clinical MR imaging

installation without the need to ramp down the MR scanner's superconducting magnet. Within the equipment room, there is a requirement for sufficient space for installation of the RF generators and cooling systems, typically one to two floor-mounted cabinet racks.

Within the treatment room, there is a requirement for space to store the MRgFUS patient table since this is typically only docked to the MRI scanner during treatments. This is often the piece of equipment requiring the largest floor space, and normally it is stored in zone 4 of the MRI suite. Additional ancillary equipment/facilities required for MRgFUS cases include an MRI-compatible vital signs monitor with capabilities for light/conscious sedation, a supply of medical air/oxygen in the suite for sedation, and local emergency infrastructure in case of an adverse reaction to the anesthetic or other patient emergency. When MRgFUS procedures are performed in a hospital, this infrastructure is typically already in place; however, in some freestanding or outpatient facilities, investment in this equipment may be necessary. The consumables associated with MRgFUS typically include acoustic coupling membranes, gel standoff pads, patient positioning aids, and degassed water for cooling and acoustic coupling. Storage space in the treatment room or immediate vicinity is necessary to keep these supplies on hand.

In the operator console area, the only additional space requirement is for a personal computer and monitor, which has the MRgFUS treatment planning and delivery software. This is typically located adjacent to or near the MRI console computer since a high degree of interaction between the MRI system and MRgFUS system operators is required during treatment. For the most part, standard MRI sequences are used for treatment planning and evaluation, with the only additional routine being the use of a gradient echo sequence for temperature monitoring using a method such as the proton resonance frequency (PRF) shift technique.

Finally, a space sufficient for preparation of patients and recovery from light sedation is necessary, preferably near the MRI area, to ensure MRI-safe supplies and equipment are used.

2.2 MRgFUS table

The central component of the MRgFUS system is the treatment table. The table docks into the MR scanner and serves as the patient support for the MRgFUS procedure. The table, similar in shape and size to a standard MRI patient table, has a built-in tank that houses the focused ultrasound transducer. The key features of this table, including the coupling fluid, MRI radiofrequency coils and gel pads, are shown in **Figure 2A**. The pre-treatment table preparation addresses appropriate acoustic coupling, patient positioning and comfort. Positioning aids are application-specific: gel pads are used to provide acoustic coupling to different anatomical targets while foam pads are used to support the surrounding anatomy. The need for customized positioning aids is more important for bone metastases applications in which targets can be at varied anatomical locations than for uterine fibroid ablation where the anatomical target is more consistently located among patients. The schematic shown in **Figure 2A** is therefore specific for uterine fibroid treatments and can be adjusted by the treating clinician and medical physicist as necessary for different anatomies and applications.

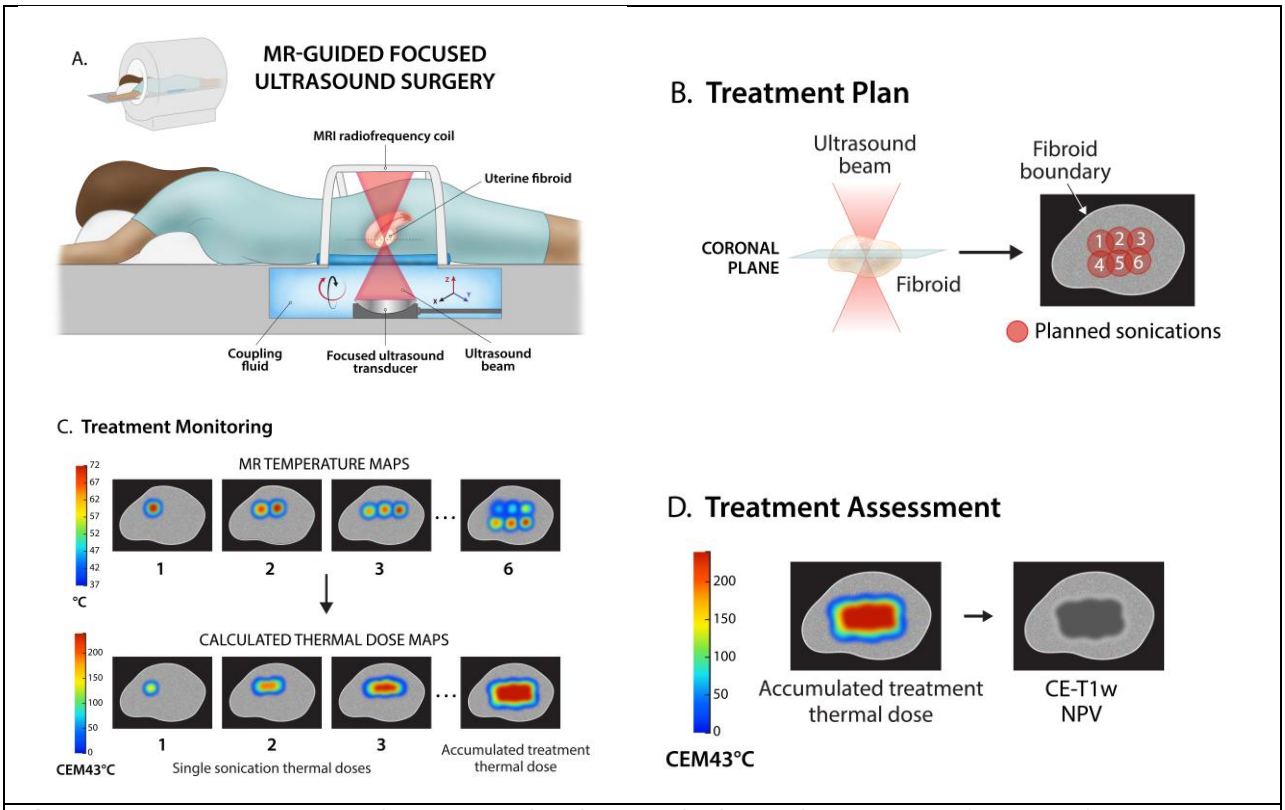

Figure 2: Key components and treatment planning, monitoring and assessment features of an MRgFUS body system. (A) Patient position in the MRI bore showing the relative positioning of a patient during a uterine fibroid treatment. Demonstration of (B) treatment planning, (C) treatment monitoring using both temperature and thermal dose maps and (D) treatment assessment.

2.3 Ultrasound transducer

All current clinical body MRgFUS systems utilize a phased-array transducer for rapid electronic steering of the ultrasound beam about the geometric focus. These transducers are spherically curved with a geometric focus located approximately 10-15 cm from the transducer surface. They are constructed from MRI-compatible materials and typically employ piezocomposites. The operating frequency is typically 1-1.5 MHz, chosen to enable deep penetration into the body while still achieving sufficient absorption to achieve the desired temperature rise at the target tissue. The size of the focus of the ultrasound beam is a function of transducer geometry, but is usually 2 mm in diameter and 8-10 mm in length, thus the transducer is capable of producing a highly localized region of thermal damage in soft tissue. Electronic steering with the phased-array transducer is used to scan this focal spot through a geometric region to heat a larger volume of tissue in a single session, either through the use of concentric circles or linear scanning (16). Electronic steering enables rapid translation of the ultrasound beam over a region approximately ±1.5 cm in extent; further translation of the ultrasound beam is accomplished by mechanical movement of the transducer in the tank. All clinical MRgFUS systems contain one or more receiver elements within the transducer for the purpose of detecting any acoustic emissions from the exposed tissue, indicative of the presence of acoustic cavitation. The signal received by these elements is converted into a frequency spectrum, and detection of broadband emissions (a signature of inertial cavitation) can be used as a control metric (17).

2.3.1 Transducer positioning system

Within the tank embedded in the treatment table, the ultrasound transducer is connected to an articulating arm under computer control that enables translation of the transducer in the x, y, and z directions (~8-15 cm range), as well as pitch and tilt control (~10-20° range) to aim the ultrasound beam into the body while avoiding critical structures such as bones and air-filled cavities (see **Figure 2A**) (18). Typically, electronic steering is used during treatment sonications under real-time MR-thermometry, whereas physical translation is used between sonications while the intervening tissue cools. In this way, physical motion of the transducer does not cause artifacts in the temperature maps since the PRF shift method is susceptible to magnetic field distortions that can arise when the transducer is moved (19). A positioning system homing procedure is generally employed during device quality assurance and system startup to ensure that all axes are functional and that the coordinate systems of the positioning system and MR are appropriately co-registered.

2.3.2 Transducer drive electronics

Each element in the ultrasound transducer array is driven by an independent RF amplifier capable of delivering power (typically ≤ 3 W continuous) at any desired phase relative to the other channels. Independent control of each element is important for several reasons. First, phase control allows electronic steering of the focus, which can enlarge the treated volume and increase treatment efficiency (20,21). Second, the ability to deactivate specific transducer elements allows the user to avoid sonicating through vulnerable structures such as the ribs, nerves or bowel (22).

The drive electronics are sited with the MR electronics and fed through filtered penetration panels into the treatment room. Since these drivers deliver power optimally for 50 Ω loads and the transducer elements have very high impedance, tunable resonant (LC) circuits are employed between them to match the load impedance to the drive electronics and transmit power efficiently. For safety, the power supply is isolated from the drive circuits via a medical grade isolation transformer.

The drive electronics are often equipped with directional power meters that measure the transmitted and reflected power. This information can be used to identify broken or underperforming transducer elements, and can even detect regions of poor acoustic coupling characterized by high measured reflected power, since a large fraction of the acoustic wave reflects back to the transducer and is converted into an electrical signal. Thus, reflected power monitoring is a component of real-time safety monitoring.

2.4 Cooling systems

Active cooling may be used for both the transducer and the patient. For the transducer, acoustic efficiency generally ranges from 40-70%, with the remaining energy dissipated as heat. Elevated temperatures in the transducer will first distort the beam and can eventually damage the transducer so energy loss (or heat) must be removed from the system. Since the front of the transducer is in a fluid bath with a large thermal mass, this surface is passively cooled. The back of the transducer, however, is exposed to air with a low thermal mass and needs to be actively cooled, generally using pumped or compressed air.

Throughout the course of an MRgFUS treatment, the skin, fat and other tissues in the near-field are repeatedly exposed to low-intensity ultrasound over a large surface area (16,23). To prevent potential cumulative thermal build up, pauses in sonication are required (24). The pause duration can be decreased through the application of active patient surface cooling. This may be

achieved by circulating cool degassed water through the ultrasound coupling medium (25) or through the use of balloons (26,27).

2.5 Treatment delivery & monitoring

The MRgFUS treatment delivery and monitoring workstation is connected to the MR scanner operator console. The treatment workstation provides three main functions: planning, treatment delivery and monitoring, accessed through a graphical user interface (GUI).

First, the operator uses anatomical MR images to develop a treatment plan. Based on daily quality assurance calibrations (see §6), the position of the transducer is overlaid on anatomical images, along with the demarcation of a focused ultrasound propagation cone. For each selected target, the beam path is identified and allows the operator to consider tissues at risk in the near- or far-field, adjusting the beam trajectory as necessary. The software can facilitate the treatment planning by filling in larger volumes with a series of smaller sonication targets (**Figure 2B**), though this process requires oversight by the operator. Different GUIs offer different tools to facilitate this process, including the ability to add tissue regions of interest (ROIs) that are sensitive and must be avoided, as well as tools to measure margins.

Second, the MRgFUS console communicates with the system hardware and positions the transducer, programs the signal generators to provide the appropriate element amplitudes and phases for the treatment plan, and initiates sonication. During sonication, the system monitors information from an array of sensors, power meters, and calculated MR thermometry images to ensure that the treatment is proceeding as predicted, abruptly halting sonication if these sensors deviate from accepted tolerances or if the patient activates a hand-held stop button because of discomfort.

Third. the MRgFUS system directs the main MR console to position thermometry slices in appropriate positions to properly capture the focused ultrasound-induced heating. Concurrently with sonication, the system receives real-time RF phase images from the MR scanner from which it calculates temperature maps (and in some cases, thermal dose) using the PRF shift method, displaying them in the form of graphs over time and real-time overlays on anatomical images (**Figure 2C**).

2.6 Key points and best practice recommendations

1. **Site requirements:** MRgFUS body systems can be deployed on standard clinical MR scanners with relative ease, though the site must be able to support additional drive electronics and permit the installation of an RF penetration panel.
2. **MRI RF coils** should be positioned with both the acoustic window and MR imaging quality in mind. Low SNR will impact treatment planning, monitoring and assessment.
3. The strategic use of **positioning aids** including pads and sandbags can facilitate acoustic coupling and enhance patient comfort.
4. **Storage space** must be considered for both FUS system components (zone 4) and the required FUS workstation (zone 3).

3: Clinical workflow for an MRgFUS treatment

The clinical workflow of an MRgFUS treatment using the clinical extracorporeal MRgFUS systems described in §2 consists of several stages, similar to radiation therapy. A typical clinical workflow diagram is shown in **Figure 3** and is described below. This workflow is appropriate to be considered when developing site-specific guidelines for soft-tissue tumor treatment or other target sites and interventions.

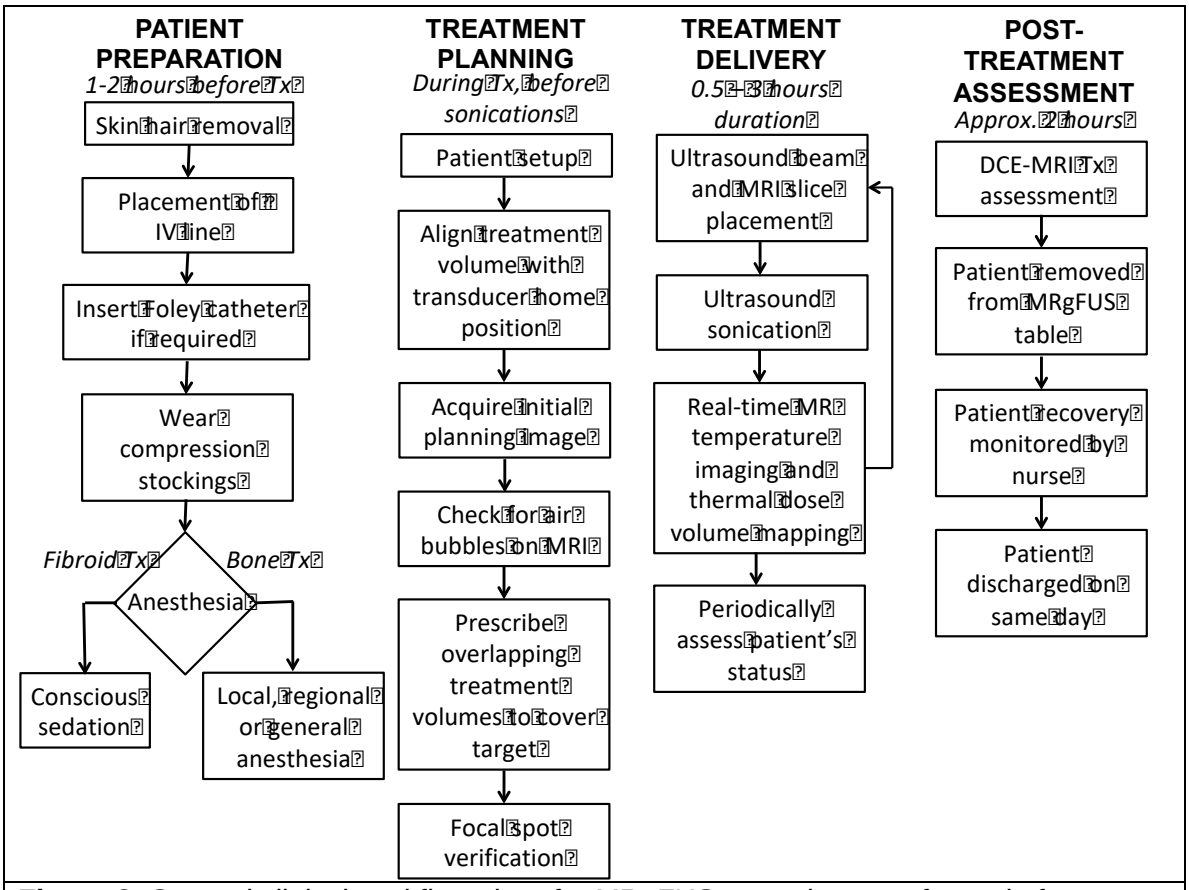

Figure 3: General clinical workflow chart for MRgFUS procedures performed after patient screening and initial assessment are completed. Typical steps for the pre-treatment, treatment and post-treatment are detailed.

3.1 Patient preparation

On the day of the treatment, each patient is instructed to report to the clinic approximately two hours before the treatment for preparation. In order to avoid skin burns and maximize beam transmission, skin hair must be thoroughly removed in the region of the acoustic window with shaving and/or depilation. If hair is incompletely removed, air bubbles may be trapped, which can result in a skin burn due to reflection of the ultrasound by air. Scar tissue in the ultrasound beam path must be avoided, as this region is also prone to unintended damage due both to increased absorption of energy and decreased perfusion. If there is an unavoidable scar present in the acoustic window, the region should be covered with a patch of acoustic reflector and/or demarcated during planning to avoid exposure to ultrasound (28). If a patient has a tattoo that is known to be MRI conditional, they may still be eligible for an MRgFUS treatment. However, it should be noted that the acoustic absorption properties of tattoo ink are unknown and therefore it is recommended to proceed with caution and to not treat through the tattoo site if possible.

An intravenous line is typically placed for the delivery of medications. A Foley catheter may be inserted into the bladder for several reasons, including to fill the bladder with saline to position the fibroid within the treatment envelope by providing an acoustic path at the lower side of the uterus, or to keep the bladder empty during treatment. Compression stockings should be worn to reduce the risk of deep venous thrombosis. Light-to-moderate conscious sedation is often

administered to help the patient relax and tolerate the stationary position and to control pain during treatment. Local, regional or general anesthesia may be needed for other treatments due to pain (e.g., treatment of bone metastases (29)). It should be noted that for some treatments it can be desirable to maintain the ability for the patient to communicate with the treatment team to provide feedback in the event pain is experienced during sonications.

3.2 Patient positioning

The ideal position for patient setup is to have the treatment target anatomy in line with the central axis of the transducer at its 'home' position and located as close as possible to the isocenter of the MR scanner bore. Successful patient setup should be assessed using three-dimensional localization MR images, to check target position and to detect the presence of trapped air in the acoustic field (see **Figure 4**). This step is often iterative and can significantly increase the length of the setup time during the procedure. It can require repositioning the patient and cleaning the skin of bubbles, or alternatively demarcating the bubbles during treatment planning to avoid passing the treatment beam through them.

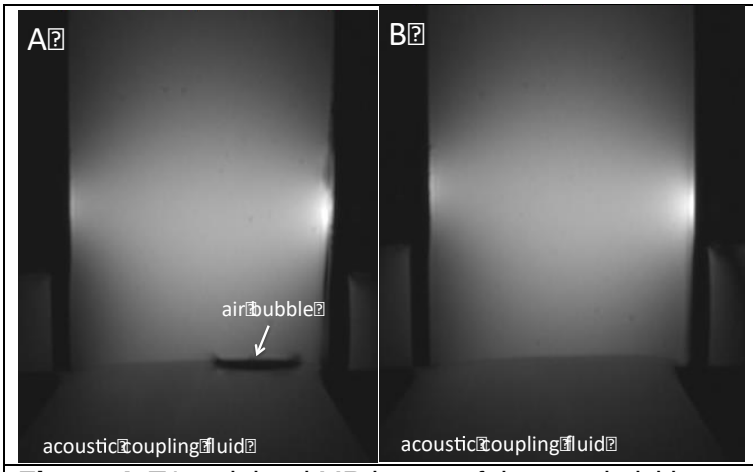

Figure 4: T1-weighted MR image of tissue-mimicking quality assurance phantom demonstrating (A) a trapped air bubble and (B) no bubbles present in the interface between phantom and the focused ultrasound transducer's water tank.

3.3 Treatment planning, monitoring and assessment

MR imaging is used throughout MRgFUS procedures for treatment planning, real-time monitoring and assessment. Both T1- and T2-weighted (T1w, T2w) images are used for treatment planning. **Figures 2B** and **2C** schematically shows how the MR images are used for the planning and monitoring of an ablation. These images are acquired as a 3D volume or in 2D multi-slice stacks in coronal, sagittal, and axial planes. Treatment planning should also evaluate the focused ultrasound beam exit locations. If required, a dispersive water coupling bolus (water bags coupled with gel) should be positioned at the beam exit area (30).

Temperature elevations during ultrasound therapy can be monitored using single-slice or multi-planar MR thermometry (**Figure 2C** schematically demonstrated single-slice monitoring) (31), with available options determined by the vendor's interface. These slices are positioned relative to the ultrasound beam, allowing for temperature monitoring and, where relevant, thermal dose

calculations at the target as well as in surrounding tissues. Real-time temperature and thermal dose maps are calculated using the proton resonance frequency (PRF) shift technique and displayed as two-dimensional color-coded overlays on top of the anatomical images, as shown in **Figures 2C** and **2D**.

In addition to treatment monitoring, MR thermometry measurements can be used to calculate the thermal dose volume (TDV) used in treatment assessment (**Figure 2D**). Thermal dose (detailed in §4) is commonly used to quantify thermal damage to tissue with values greater than 240 cumulative equivalent minutes (CEM) at 43°C indicating ablative exposures. The TDV indicates the volume of tissue that has reached a thermal dose sufficient for ablation. This volume can be overlaid on the treatment planning or monitoring images. Treatment assessment also includes acquisition of post-treatment T2w fat-saturated images followed by T1w fat-saturated sequences acquired after administration of clinically approved gadolinium-based contrast agents. T2w images may demonstrate an increase in the signal intensity of the treated target as a sign of successful treatment (32). In addition, these images can be used to assess edema or damage in the tissues surrounding the target. An example of a T2w image before and immediately after an MRgFUS treatment of a left iliac bone metastases is shown in **Figure 5**.

Unintended tissue damage can occur during MRgFUS treatments. First-, second- and third-degree skin burns are theoretically possible (30). Typically, first-degree burns are treated with no follow-up required. Second- and third-degree burns are treated and monitored for further progression. If there is damage to tissues surrounding the target, rest is typically prescribed for one to four weeks to allow recovery and healing. For the treatment of uterine fibroids, the contrast-enhanced T1w images are utilized to assess any remaining perfused, viable tissue in the target (**Figure 2D**). The non-perfused volume (NPV) can be calculated from these images, providing a measure of the effectiveness of the treatment. For example, the NPV ratio predicts uterine fibroid symptom relief (33).

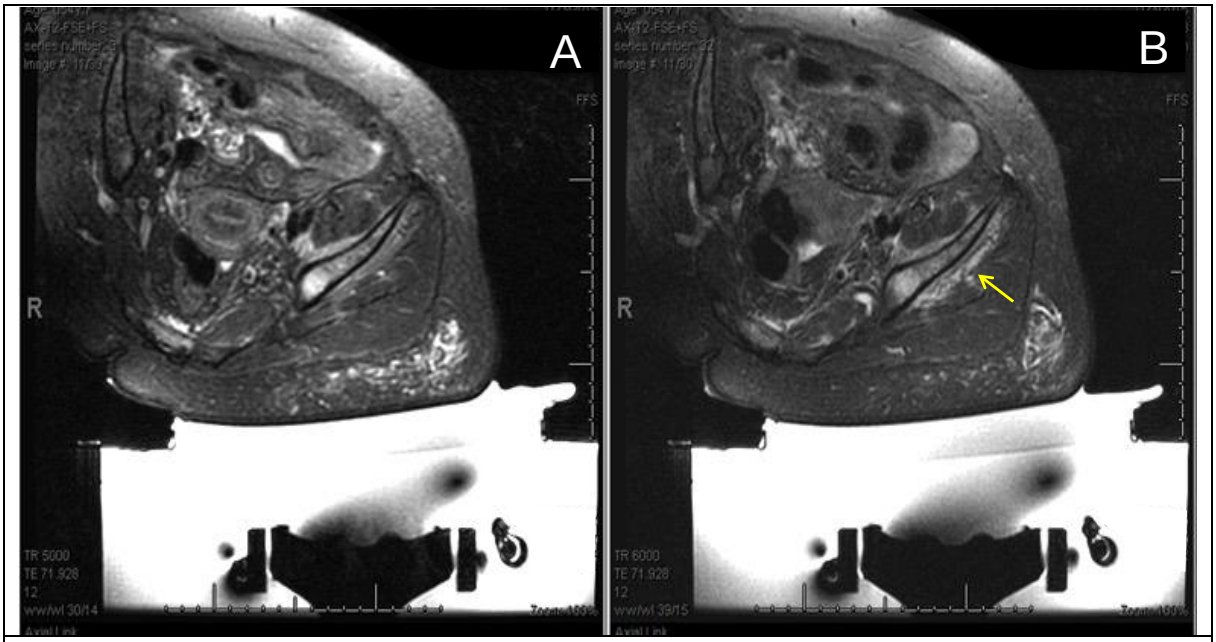

Figure 5: A comparison of T2w MR images (A) before and (B) immediately after MRgFUS treatment, showing edema (arrow) superficial to the treated left iliac bone metastasis.

3.4 Integrated procedural safety steps

There are several safety checks that should be integrated into all phases of an MRgFUS treatment beyond the routine safety measures of MRI. During the treatment-planning phase, each planned sonication is analyzed based on the expected energy density on the skin, as well as on other low-energy density contours drawn during treatment planning to demarcate the bowel or sacral bone, for example. This safety check allows the operator to alter individual sonications during treatment planning to minimize potential damage to other structures outside of the target by translating or tilting the transducer, or by reducing the planned sonication size or energy. After planning, verification sonications are performed in at least two planes with non-ablative energies in order to make final minor adjustments in alignment prior to treatment; this allows for patient-specific adjustments that account for the thickness and types of tissues traversed to the target. A thermal dose verification sonication is also performed to aid in determining whether the energies predicted for sufficient thermal dose accumulation are too high or too low. This is needed because temperature elevation is not only a function of energy, but also a function of complex heat transfer in tissues (detailed in §4).

During treatment, individual sonications are assessed first using a reflection test to confirm that nothing is impeding the ultrasound beam from reaching the target. Each sonication is also monitored for movement by comparing the location of fiducial markers placed on planning images with real-time images obtained during heating. In addition, a periodic movement detection scan is also used to automatically compare the current location of the targeted tissue with the location drawn on pre-operative images. MR thermometry magnitude images are an additional means to detect motion by comparing the contour placed during planning around the region of treatment to the tumor margin visualized during treatment. These MR thermometry images are the most important safety indicator, as they are used to confirm that heating is occurring predominantly in the target and not at another location, such as on the skin, or on nearby bowel or nerves. Non-focal heating is always possible within a single sonication or as the result of heat accumulation during multiple consecutive sonications. As a final safety step, cavitation is monitored continuously during each sonication. An operator-activated button on the workstation can be used to stop individual sonications if movement, off-target heating, or cavitation is detected. It should be noted that patient feedback is also an important safety indicator, since sensations of excess warmth or nerve stimulation can often be experienced by a patient before these effects are apparent on imaging.

3.5 Key points and best practice recommendations

1. **Skin preparation**: Skin hair must be thoroughly removed in the region of planned ultrasound exposure. Scars in the treatment region must be avoided to prevent excessive energy absorption that may result in burning of the skin.
2. **Far-field protection**: Beam exit points need to be considered, and if appropriate a dispersive water coupling bolus (water bags coupled with gel) should be positioned at the beam exit area to minimize far-field tissue damage.
3. **Patient motion:** Patient and organ movement should be tracked throughout the procedure through a combination of fiducial markers and real-time images. Patient motion is a major source of treatment uncertainty that must be managed by the medical physicist.
4. **Non-focal heating:** Out-of-target excessive heating is always possible during single or multiple sonications. MR thermometry images are the most important safety indicator to confirm that heating is occurring predominantly in the target and not at another location.

4: Quantitative metrics, data types and terminology

The ability to characterize, predict, and control the effects of ultrasound on tissue is made possible by quantitative knowledge of specific properties of the ultrasound field and the tissues. The assessment of acoustic, thermal and mechanical tissue properties is beneficial for all aspects of MRgFUS therapies. While official standards for therapeutic MRgFUS systems are still developing, rigorous system assessment should be performed with a set of quantitative metrics subsequently reported. These metrics can assist in the calibration, quality assurance and long-term maintenance of MRgFUS systems and allow for improved comparison of MRgFUS studies. This section formalizes these quantitative metrics in support of further efforts to standardize the quality, reliability and predictability of MRgFUS treatment results.

4.1 Acoustic Parameters

While direct measurements of transducer ultrasound characteristics can be obtained in water, accurate estimates of *in situ* acoustic properties are necessary to adequately characterize the interaction between ultrasound and tissue on a patient-specific basis. Most of these properties cannot be measured at clinically applied intensities due to the limitations of the measurement equipment. While the minimum requirements for the reporting of acoustic parameters for both diagnostic and therapeutic applications have been clearly outlined in other work (34), a summary of the many properties of the ultrasound field and transducer are detailed herewith. A more complete listing of descriptive parameters can be found in the International Electrotechnical Commission Draft Technical Specification on High Intensity Focused Ultrasound (IEC/TS 62556 Ed. 1.0) (35).

Ultrasound beam properties: The effects of ultrasound on tissue depend on the local distribution of the ultrasound pressure, as well as on the acoustic and thermal properties of the tissues. The frequency (*f)* of the ultrasound is a characteristic of the oscillating source while the wavelength (λ) of the ultrasound beam in a particular medium is defined as the speed of sound in that medium divided by the frequency. The energy carried by the ultrasound is usually described in terms of the energy density (J/m^3) or the intensity (W/m^2), which is proportional to the square of the pressure amplitude. Commonly referred to transducer properties are summarized in **Table 1**, and described below.

Table 1: Typical MRgFUS transducer characteristics

Transducer Characteristic	**Characterization Method**	**Relevance**
Aperture (*D)*	Physical dimensions of transducer front face	In general, the size of the focal spot is inversely proportional to the aperture size.
Focal Length (*L*)	Transducer geometry quantification	Distance of transducer face to geometric focal point. For a spherical transducer, this is the radius of the sphere.
Element Configuration (N_{elem})	Defined by transducer design.	Single element transducers must be mechanically translated to move the focal point. Phased-array transducers provide electronic steering allowing for multi-focus and volumetric ablation.
Frequency (*f*)	Driving frequency of the transducer element(s)	Affects both the wavelength and attenuation of the ultrasound beam. The frequency of a HIFU system is application dependent.
f-Number (*f#*)	*L/D*	The ratio, *L/D*, is defined to be the *f-number* (*f#*) of the transducer; the smaller the *f#*, the smaller the focal spot increasing the energy deposited at that point.

Beam Full Width Half Maximum (*FWHM*)	Hydrophone measurement	The width of the beam measured at the focal point, assessed with either pressure or intensity (should be specified).
Efficiency	Radiation force balance or hydrophone scans of intensity over full cross-sectional area of the ultrasound beam	Defines the relationship between electrical and acoustic power. A greater efficiency will result in a higher acoustic output for a given electrical input.

4.2 Acoustic field descriptors

Pressure distribution: The pressure distribution in tissue is a function of the transducer characteristics and tissue properties, and determines the spatial pattern of heating in tissue. Pressure distribution measurements are usually made using hydrophone sensors that scan the field in free-field conditions in water. The mapping of pressure distribution measurements in water to corresponding estimates in tissue requires the inclusion of parameters that relate to ultrasound propagation in tissues. The process of including energy losses due to propagation in lossy overlying tissues is referred to as derating. Typically, either free-field or estimated *in situ* pressure is reported as the compressional pressure (*P*+), also defined as the spatial-peak temporal-peak pressure (P_{SPTP}), as well as the peak rarefactional (*P*-) or peak negative pressure (P_{NP}), as illustrated in **Figure 6A**. If estimated *in situ* values are reported, the derating method applied with a worked example should be provided (34).

Acoustic power: Ultrasound is typically created by applying electrical voltages to the piezoelectric elements of a transducer. The conversion of electrical power to acoustic power is a function of the electromechanical efficiency of the transducer, driving electronics and the coupling to the medium. While several measurement techniques for characterization of the ultrasound beam exist (36), radiation force balance and hydrophone measurements are more widely implemented. For example, the total acoustic power can be measured by a radiation force balance apparatus (37) or hydrophone scans of intensity over the full cross-sectional area of the beam (see §8.2).

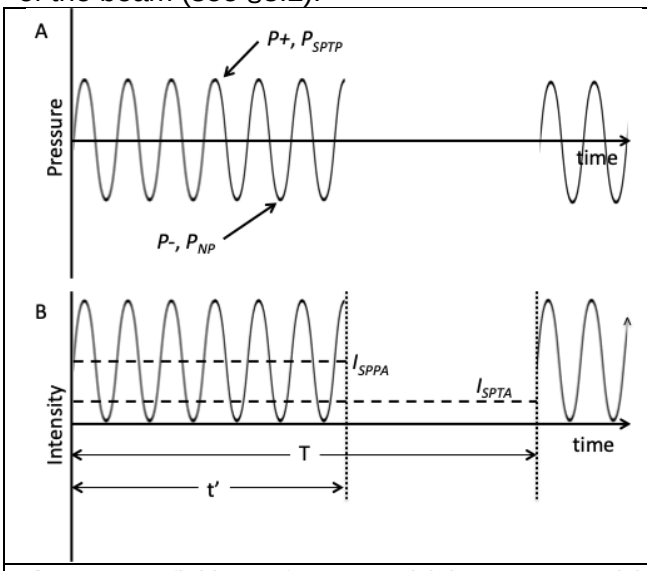

Figure 6: Definitions of measured (A) pressure and (B) intensity values commonly used in high intensity focused ultrasound. While MRgFUS for many procedures is applied in a continuous wave mode (t'=T), it can also be applied in a pulsed mode with a t'/T duty cycle.

Intensity: The acoustic intensity distribution can also be measured using a sensitive hydrophone, consisting of a point sensor that is mechanically scanned through the ultrasound field. Accuracy in measurement depends on the hydrophone effective active element radius being comparable with or smaller than one quarter of the effective wavelength of the ultrasound in water to avoid spatial averaging errors, at least for the fundamental frequency (35). However, even if this condition is not met or if the pressure wave has significant harmonic content (as is commonly true), an inverse filter method exists for correcting for spatial averaging loss across the hydrophone sensitive element for the fundamental and all harmonics (38). (Note that the harmonic beam width decreases with frequency (38)). To account for the fact that the intensity is highly localized and the ultrasound may be pulsed, the IEC/TS 62556 report lists several different intensity parameters, including:

a) I_{SAL}: the spatial average intensity, linear conditions. This is the intensity spatially averaged over the area enclosed by the half-pressure-maximum contour in the plane containing the focal point (for focusing transducers) or beam maximum (for non-focusing transducers), as determined under linear conditions;
b) I_{SPTA}: the spatial-peak temporal-average intensity. This is the maximum value of the temporal-average intensity in an acoustic field or in a specified plane;
c) I_{SPPA}: the spatial-peak pulse-average intensity. This is the time average of the maximum intensity at a particular point in an acoustic field over a single pulse.

Although beyond the scope of this report, acoustic non-linear propagation (i.e., finite amplitude distortion) may be possible under certain conditions. The practical main effect is the rapid derating of acoustic pressure leading to cavitation and/or accelerated pre-focal lesion formation and growth (39).

4.3 Tissue acoustic properties

Whereas water is isotropic and has a low attenuation coefficient, tissues have internal structure and characteristics that modulate the beam propagation. Quantitative properties used to describe the propagation of ultrasound through tissue are speed of sound, impedance and attenuation coefficient. Acoustic attenuation is used to estimate the *in situ* exposure levels during a treatment and more accurate values will result in improved derating schemes, which should always be reported when applied. While acoustic properties are not directly measured or typically reported in clinical studies, they directly impact parameters that are achieved clinically. A summary of these properties with typical characterization techniques is found in **Table 2** and detailed below.

4.4 Cavitation

Acoustic cavitation occurs when MRgFUS is applied at high pressure amplitudes, leading to the excitation of microbubbles. Stable cavitation occurs when the bubbles oscillate and emit harmonics and sub-harmonics of the excitation frequency. Inertial cavitation can occur during MRgFUS therapy when the rarefactional pressure exceeds the cavitation threshold of the target tissue. Cavitation can be detected using a passive acoustic detector (e.g., hydrophone) that can assess the resulting broadband acoustic signals. Passive cavitation detectors are integrated into MRgFUS systems and used to monitor the cavitation activity during HIFU treatments (40,41).

Property	Characterization method	Relevance
Density (ρ)	Water-displacement	A determinant both of acoustic impedance and thermal diffusivity. Typically 1000 kg/m^3 ± 10% for most soft tissues.
Speed of sound (c)	Through-transmission	A determinant of acoustic impedance and wavelength. Typically 1500 m/s ± 10% for most soft tissues.
Attenuation (α)	Through-transmission or reflection technique	Encompasses both absorption and scattering components. Absorption determines the amount of heat absorbed in a tissue. This is a function of transducer frequency. Values can change during an MRgFUS treatment (42,43).
Impedance (Z)	$Z = \rho c$	Impedance differences at tissue boundaries dictate reflected and transmitted wave magnitudes.
Non-linearity parameter (B/A)	Finite amplitude insertion substitution method (44-46)	Describes the level of non-linearity for a tissue, where A & B are the 1st and 2nd Taylor series expansion values for the relationship between pressure and density. Of particular importance for high-pressure amplitude applications.
Thermal conductivity (k)	Typically use table values. Can use an invasive probe technique to directly measure values (47,48)	Tissue-specific transport property that determines how well tissue can conduct heat. Fat has a lower conductivity than other soft tissues, resulting in an insulating response.
Specific heat (c)	Typically use table values but can be determined using a calorimeter	Measures the ability of a tissue type to store thermal energy. Typically most tissues have a specific heat value lower than water (4186 J/kg*K).
Perfusion (W)	Both table values (49) and tissue-specific estimation techniques (50,51) are available in the literature	Defined as the process of blood delivery to a tissue's capillary bed. Reported values for perfusion vary widely across tissues and are known to change dynamically during treatment. Represented as a scalar term in the oft-used Pennes bioheat transfer equation (52). Large vessels can cause a 'heat-sink' effect.

4.5 Thermal properties

As ultrasound passes through the tissues, a fraction of the energy is absorbed as heat. The rate at which heat is absorbed is given by:

$$Q = \frac{-\partial I}{\partial x} = 2\alpha I$$

where Q is the rate of heat deposition (W/m^3), α is attenuation (Np/cm*MHz) and I is ultrasound intensity (W/m^2). Q becomes the driving function for the distribution of heat and resulting temperature change in tissue. The subsequent conduction of heat through the tissues then depends on the tissue thermal properties. Even if a thermal mechanism is not expected in an MRgFUS treatment, the temperature rise due to an acoustic exposure should be either measured or estimated whenever possible (34). While knowledge of the tissue thermal properties is necessary to estimate the thermal effects of any ultrasound exposure, it is also known that thermal properties change throughout a therapeutic thermal treatment (53,54). This variability should be acknowledged in all treatment planning and modeling efforts. A summary of key thermal properties is found in **Table 2**.

Table 2: Tissue acoustic and thermal properties

4.6 MRI measurements

MRI provides a highly useful tool for the *in situ* evaluation of the interactions of focused ultrasound with tissue. Although ultrasound parameters can be measured directly in water using either a force balance or hydrophone, such instruments cannot be used conveniently in tissues. Fortunately, interactions of ultrasound with tissues produce effects that can be detected with MRI. The absorption of acoustic energy in the tissues may result in local temperature increases which are sufficiently high to be detected as changes in MRI parameters that are sensitive to changes in temperature, including the proton resonance frequency (PRF), longitudinal and transverse relaxation times (T1 and T2), and the apparent diffusion coefficient (ADC). PRF is based on hydrogen bonding (55-57) and is the most commonly used method of measuring temperature with MRI and typically achieves precision of ±1°C clinically, but it is not sensitive to temperature change in fat. Both the longitudinal relaxation time T1 and the transverse relaxation time T2 have been used recently to monitor temperature changes in fat during MRgFUS treatments (58-61). Diffusion weighted imaging has also been used to make measurements of temperature changes (31,62). Excellent reviews of MRI temperature measurements using these parameters have been given elsewhere (31,63,64).

4.7 Treatment assessment

While there is a large amount of literature describing treatment outcomes from a number of input quantities, currently there is not a direct relationship between a known ultrasound or thermal dose quantity and a defined *in vivo* biological effect. This issue of creating a dosimetric framework for therapeutic applications has been investigated thoroughly by Shaw et al. (65).

Thermal Dose: The concept of a thermal dose is derived from studies that noted an exponential relationship between temperature and time for a given isothermal effect (66). It is typically assumed that tissue necrosis occurs at 240 CEM at 43°C, although it has been documented that tissue-specific thresholds exist (67,68). In MRgFUS, spatially varying thermal dose distribution and the resulting thermal dose volume (e.g. tissue that has achieved 240 CEM 43°C) are derived from the MR temperature measurements and are therefore a function of temperature measurement accuracy.

Contrast enhancement imaging: Contrast-enhanced MR imaging (CE-MRI) is the most commonly used technique to assess the effects of MRgFUS treatment. T1w CE-MRI images are used to calculate the NPV in uterine fibroids and tumors after all ablations have been completed (§3.3). However, the literature documents both under- and overestimations of calculated NPV when compared to the thermal dose volume (69-72). In addition CE-MRI does require the injection of a gadolinium-based contrast agent. If the treating clinician desires to increase the ablation volume after the injection of the contrast agent, errors in the MRI thermometry could be introduced. There is also the possibility that the gadolinium-based contrast agent could become retained in the tissue (73). Using multiparametric MRI protocols to acutely assess MRgFUS treatments have shown some promise, but applying them in a clinically feasible time frame remains a challenge (74). MRgFUS can cause several types of treatment effects and there are several potential metrics that could measure these effects. However, any MRI method used must be validated in multiple tissue and tumor types in order to fully characterize its potential to assess MRgFUS treatments.

4.8 Key points and best practice recommendations

1. **Tissue properties**: While tissue properties cannot be directly measured *in situ*, knowledge of the expected values for particular tissues is important for MRgFUS treatment planning. In addition, it is known that these properties can change during MRgFUS procedures, affecting the treatment outcome.
2. **Acoustic exposure reporting:** Acoustic exposure parameters should be reported according to published best practice guidelines (34) to better enable study comparisons and data correlation.

5: Sources of Uncertainty

Uncertainty in MRgFUS arises from uncertainty in the direct and indirect assessment of the desired pathological outcome. Therefore, a medical physicist should be cognizant of the variety of uncertainties that can interfere with the execution of the MRgFUS procedure as well as methods that can be employed to minimize or avoid them (75).

5.1 Pathologic margin

Because the focal point in MRgFUS is usually smaller than the overall target volume, the process must be repeated multiple times to deliver an effective therapy. Similar to radiation therapy as well as other thermal ablation techniques, the lack of direct pathological margin assessment during treatment and the need to define and assess these boundaries with MRI contributes to the uncertainty in both delivery and outcomes. For example, since the penumbra of an MRgFUS exposure can be very sharp (§2.3), the placement of the boundary of a target volume is critical since any resulting tissue damage margin will be very abrupt beyond that boundary (76). Target volume planning will therefore depend on the MR image resolution and the ability of the MR image contrast to reveal target boundaries. Both of these metrics are a function of the MR signal-to-noise ratio available for a particular treatment. Similar to radiotherapy, higher quality imaging will result in improvements to the definition of the gross tumor volume, the clinical target volume and the planning target volume (77), ultimately providing better outcomes in MRgFUS therapy.

5.2 Treatment planning

In the absence of the ability to directly monitor the tissue pathologic response during treatment, knowing the distribution of heat delivered during treatment provides a nearly direct assessment of treatment outcome. Careful attention to treatment setup is necessary to minimize barriers to treatment delivery (e.g., air interfaces, bone), as ultrasound propagation in tissues is inherently more sensitive to organ and tissue boundaries than the radiation beams used in radiotherapy. Protective measures to ensure safe delivery are often required (§3). Although unlikely to satisfactorily replace treatment monitoring, patient-specific prospective planning can be useful to assess potential barriers that may affect successful MRgFUS delivery to a target volume. While standard property values are typically used in treatment planning, knowledge of the parameters influence on treatment outcome is essential when interpreting planning results.

Attenuation: Unexpected differences in tissue attenuation along the beam path can lead to power loss or gain at the focus and unexpected heating near the target volume. Examples include gas in the coupling fluid, scar tissue, calcifications, bone, cavitation generation and increased attenuation due to changes in tissue temperature or non-linear propagation (42,78).
Speed of sound: Beam dimensions and focusing characteristics tend to be made based on an assumed speed of sound. Deviations from this ideal can lead to focal location errors and power loss at the focus from phase aberration. Examples include propagation through thick adipose fat layers, fluid-filled bodies or coupling pads not specifically designed for ultrasound propagation and the ‘thermal lens’ effect at the focus due to temperature-dependent speed of sound.

Non-linear propagation: Non-linear effects of ultrasound propagation in tissue contributes to cavitation generation as well as the emission of higher harmonics, which can change the expected energy delivery in the focal region (39).
Acoustic impedance: Assessment of interfaces with different acoustic impedance values is a critical component of planning and patient-positioning assessment. Reflected energy can result in heating in unexpected locations and/or loss of power at the focus.
Anatomy: Patient-specific anatomy and patient positioning limitations and constraints can result in non-normal ultrasound beam incidence causing beam refraction, potentially resulting in power loss or focal positioning errors.

5.3 MR temperature imaging

Due to the uncertainties present in treatment planning, techniques for monitoring the delivery of energy into the patient are desired to ensure both safety and efficacy. MR temperature imaging (MRTI) has the unique ability to accurately assess the distribution of temperature change. As described in §4.7, MRTI provides a powerful *in situ* dose measurement during therapy, but is susceptible to uncertainties from multiple sources. Errors in tissue temperature estimation (79), discrete sampling errors (80), as well as the appropriateness and accuracy of the model for predicting the isoeffect in a specific tissue are all propagated into this step. MRTI measurements are typically used to determine the endpoint for a single MRgFUS exposure, making proper understanding, quantification, and management of MRTI uncertainties critical in MRgFUS treatments.

The accuracy and precision of MRTI is dependent on several factors. The overall signal-to-noise ratio of the phase images used to calculate temperature change is a function of common sequence parameters including repetition time, echo time, bandwidth, and the use of parallel imaging. The type of radiofrequency MRI coil used and its placement with respect to both the patient and the MRgFUS transducer significantly affect SNR. While in MR imaging it is desirous to place the coil as close to the imaged anatomy as possible, this is often very difficult in MRgFUS therapies due to the presence of the required MRgFUS system hardware.

The temporal and spatial resolution of the MRTI measurements can also affect the accuracy of predicting the outcome of the treatment. Resolution requirements will be a function of the properties of the heating pattern. For example, if single-point sonications are performed, a voxel size of approximately 1.0 x 1.0 x 3.0 mm^3 would be required to accurately measure the temperature while volumetric sonications (e.g., a 4-mm diameter circle) could be accurately measured with a larger voxel size (e.g., 2.0 x 2.0 x 5.0 mm^3) (80). The imaging spatial resolution must adequately capture the heating dynamics present in both the axial and longitudinal directions of the ultrasound beam. The optimal orientation and configuration of the slices are a function of the ultrasound beam characteristics and the necessity of monitoring the near- and far-fields of the treatment. Because MRgFUS can heat tissues at the rate of 1°C/second, the temporal resolution must be such that this heating rate can be monitored to limit overtreatment.

While the temperature sensitivity coefficient for water is known to be -0.01 ppm/°C, it is tissue-type dependent. While most studies have found values between -0.009 and -0.01 ppm/°C, other studies have found different values (79). This potential uncertainty should be considered when validating treatment assessment techniques.

Several artifacts are common with MR thermometry. Drift of the external magnetic field, which can be exacerbated by high gradient use (81), can result in what is commonly referred to as

phase drift. This drift can cause errors in temperature measurements but can be corrected through the use of reference phantoms (56,82) or specialized reconstruction methods (83). Local magnetic field variations can also affect the accuracy of MR temperature measurements due to the temperature dependence of the susceptibility constant, which is tissue-type dependent (84). The large temperature-dependent change in fat susceptibility can cause considerable errors in MR temperature measurements (±6°C). Because of this and the approximately 3-ppm resonance frequency shift difference of water hydrogen and those of the dominant fat hydrogen resonances (adipose and bone marrow), most MR temperature imaging methods use fat saturation to eliminate the fat signal. Finally, motion can severely affect MR temperature imaging accuracy, as discussed in the following section.

5.4 Motion and compensation strategies

All types of physiological motion are a major source of uncertainty in MRgFUS with respect to both energy delivery and therapy guidance, as demonstrated in **Figure 7**. In this example the measured temperature change is corrupted due to the muscle movement in a rabbit thigh during the ablation procedure. It is therefore important to differentiate between the sources and the time-scale of the different types of physiological motion and the potential correction methods.

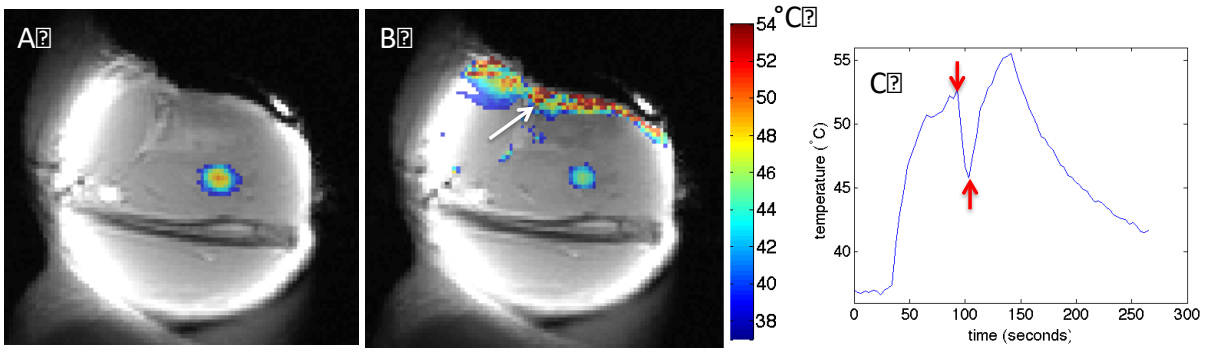

Figure 7: MRTI temperature error due to spontaneous muscle movement in a rabbit thigh. (A) and (B) show coronal slices of a single MRgFUS sonication, with spatially inaccurate temperature measurements demonstrated in (B). (C) The motion can be seen in the temporal data in the temperature versus time response of a single voxel. The rabbit spontaneously moved approximately 100 s into sonication resulting in an artificial drop in temperature response (red arrows in C) and white arrow in (B).

Respiratory motion: The liver and the kidney of an adult patient move under free-breathing conditions with a periodicity of around 3-5 s, and amplitude of 10-20 mm. While the motion pattern of free-breathing patients is periodic over longer episodes (<30-45 s), it is frequently subject to changes in amplitude, phase and frequency before a new stable breathing rhythm is reached. In particular, the occurrence of involuntary spontaneous motion events, such as swallowing, coughing or muscle spasms, is hard to predict and interrupts a regular breathing pattern. The influence of respiratory motion during the initial and the final phases of the MRgFUS procedure are generally addressed with the established measures of diagnostic MRI: either respiratory gating or breath holding. Several approaches have been investigated to address respiratory motion, including induced apneas (85,86), gating strategies (87-89), beam steering strategies (90), MR-based tracking (91-97) and US-based tracking (98,99). In addition the motion of moving targets will modify the local demagnetization field, and thus also the local magnetic field, experienced by the target organ. This will also result in temperature artifacts (56,100). While several techniques have been proposed to compensate for these motion-related

errors (91,101-107), none of these techniques have been implemented clinically to date.

Peristaltic motion: A second important source of physiological motion is induced by peristaltic and digestive activity. Although the timescale of peristaltic motion events depends on the particular source, the resulting abdominal organ position shifts usually occur on a scale of several minutes (108,109) and are generally non-reversible and aperiodic. Peristaltic motion can clinically be moderated by several measures including diet modification (110) administration of an antispasmodic (111) and the use of Foley catheters (108).

Spontaneous motion: Finally, spontaneous motion is considered one of the most challenging types of physiological motion since it occurs infrequently, on a very short time-scale and is, in general, irreversible. It is particularly problematic for long interventions that require the patient to remain in an uncomfortable position. Similar to the field of external beam therapy, this problem has been alleviated by using restraints (112), sedating the patient (113), or introducing general anesthesia.

Tissue swelling that occurs during treatment can cause uncertainty to both the definition of the volume for treatment as well as quantifying the cumulative volume already treated (114). The changes in tissue volume due to thermal ablation are perhaps more immediate due to the local inflammatory response generated by this type of tissue injury.

5.5 Thermal dosimetry

While thermal dosimetry is a widely used concept and is used clinically for MRgFUS, there are several issues concerning its use in MRgFUS therapies. First, while it is typically assumed that tissue necrosis occurs at 240 cumulative equivalent minutes at 43°C, it is known that tissue-specific thresholds exist (67,68), thus requiring some kind of weighting scheme to be defined. Second, the original derivation was performed at temperature levels between 42 and 47°C, well below those typically encountered in MRgFUS clinical treatments. In addition, there is no consideration of potential mechanical effects including cavitation and radiation forces. Despite these drawbacks, the ability to measure temperature with MRI, thus enabling the calculation of thermal dose, does provide some insight into the efficacy of the treatment. It should be noted that artifacts in the temperature measurements have a large impact on the precision of the thermal dose estimate due to its exponential dependence on the temperature.

Three-dimensional isotropic MR-thermometry in a large field-of-view would provide an accurate monitoring of the thermal dose measured in the targeted area, as well as any collateral damages (such as edema induced in the near-field close to the skin or due to heating of the bone by absorption of the acoustic energy). An inherent trade-off exists between the available signal-to-noise ratio (SNR), spatial resolution, volume coverage and scan time. While several kinds of volumetric thermometry have been investigated (102,115-117), no 3D MRTI is currently used clinically.

Thermal dose is generally calculated assuming that the tissue in the treatment region returns to 37°C between sonications. However, when the baseline is determined from the previous sonication, the larger, predicted thermal dose volume was found to have better agreement with the NPV assessment (118). In addition, it has been demonstrated that a significant amount of thermal dose accumulates during the cooling phase of the sonication and more accurate thermal dose measurements are achieved when both the heating and cooling phase of each sonication are used to calculate the cumulated thermal dose (118). Gradual organ shift can also occur during treatments, causing misregistration in the cumulative thermal dose maps from

each sonication. Organ tracking and registration can be implemented to correct for this potential error.

5.6 Key points and best practice recommendations:

1. **Motion:** Intra- and inter-scan motion can impact all aspects of an MRgFUS procedure. Clinical protocols should include appropriate treatment margins based on anatomical locations and be able to adapt to potential motion artifacts on a patient-specific basis during the treatment planning, monitoring and assessment phases.
2. **Treatment assessment:** Procedure uncertainties, including temperature measurement and subsequent thermal dose calculations, should be considered when assessing the treatment outcome.

6: Safety and quality assurance

A formalized program that provides quality assurance (QA) of expected device operation and safe clinical operation is a critical component of any medical technology. In the case of MRgFUS, QA takes on heightened importance due to the technical complexities of the system, the diversity of potential indications, known uncertainties present in each procedure, and the possibilities for adverse clinical outcomes if the system is not working within specifications. When starting an MRgFUS program, it is essential that the entire institution, from administration down through the treatment team, support a robust quality assurance effort to help mitigate against risk to the patient and provide the most effective and positive clinical experience for both the patient and for clinical personnel.

There are many components to a well-designed quality assurance program, including a formal risk-analysis of the clinical workflow, pre-shipment testing of equipment by the manufacturer, acceptance and commissioning activities when the equipment is installed at an institution, and periodic quality assurance of various aspects of the system that may have an important effect on the technical operation or clinical outcomes of a procedure.

6.1. Pre-shipment testing

Currently available MRgFUS systems are developed as an integration of therapeutic ultrasound units with diagnostic MR units. Many aspects of these systems are difficult to test in an integrated fashion after installation, as this requires in-depth engineering information that resides with the manufacturer. Manufacturers have a responsibility to follow recognized good manufacturing practices (119) and follow accepted national and international standards where they exist. It is also incumbent on the manufacturer to test aspects of the equipment that cannot be evaluated on site due to integration challenges or to the presence of high-strength magnetic fields. The pre-shipment testing results obtained by a manufacturer should ideally be reported to the customer institution before shipment.

6.2. Risk analysis of clinical procedures

Institutions involved in MRgFUS procedures should commit to performing formal risk-based analyses of the clinical procedure(s) to be followed for a given indication. Formalized risk-analysis is a well-established technique in manufacturing, and is gaining prominence in medical settings. The recently published report of AAPM Task Group 100 (120) provides detailed guidance for modeling a clinical process, formalizing an analysis and prioritization of process risk (based on severity, frequency, and ability to detect a fault), determining methods for

mitigating risk in priority order, and evaluating the effectiveness of implemented process changes. This important step forms the backbone of any quality control/improvement effort, and requires the multidisciplinary participation of each member of the clinical treatment team.

Risk-based process analysis is especially important for an emerging field such as MRgFUS, where the technologies and techniques are changing rapidly, and the most appropriate QA tests, frequencies, and passing criteria are not well established. Formalized methods for analyzing a clinical process make it possible to determine which areas of risk are best managed via detection (i.e. QA tests), and which are best mitigated through changes in the clinical workflow that eliminate or reduce the risk. Periodic review of the risk analysis can help to determine appropriate QA frequencies and QA pass criteria that are based on data rather than an instinctual notion of what is reasonable to expect. An example of the application of failure mode and effects analysis (FMEA) to an ultrasound hyperthermia cancer therapy system has been reported (121).

6.3. Equipment acceptance and commissioning

Acceptance and commissioning are two closely related quality assurance tasks that provide a formal method for evaluating new equipment and creating a baseline characterization of system performance that can subsequently be tracked over time.

Acceptance Testing: Every MRgFUS device should undergo formal acceptance tests with defined pass criteria. The purpose of acceptance testing is to ensure that new equipment meets its intended design specifications. Acceptance tests and criteria are generally developed by the manufacturer and are commonly included as part of the sales contract of the equipment. Ideally the institution should have input into the acceptance procedures, tests to be performed, and the definition of a successful test.

In the case of MRgFUS systems, there may be several levels of acceptance tests. The MR and focused ultrasound subsystems may have separate acceptance tests (122), and then there may be acceptance tests for the integrated system (123). Ancillary equipment such as auto-injectors, monitors, and other clinical equipment may have their own acceptance testing criteria. Acceptance testing is often performed by the manufacturer under the observation of a qualified medical physicist.

While the details of acceptance testing for a complete MRgFUS system will necessarily vary with manufacturer, some common tests would likely include:

- Test of motor systems and their capability to move the transducer to desired locations
- Test of transducer focusing and beam steering (using MR thermometry or other methods, such as field mapping using a hydrophone)
- Test of table position and homing within magnet
- Measurement of magnet stability and baseline temperature stability
- Evaluation of imaging SNR and quality using appropriate MRI RF coils (in phantom and volunteer)
- Evaluation of temperature accuracy in phantom – comparison of MR thermometry against fiberoptic temperature sensor
- Function of planning/delivery software
- Cavitation detection software/electronics
- Safety interlocks

Commissioning: Commissioning is a QA task that is distinct from acceptance testing. The purpose of commissioning is to establish a comprehensive baseline characterization of system performance that will be used as a reference for comparing measurements of ongoing periodic quality assurance tests to make it possible to detect changes in system performance. Unlike acceptance tests that are often performed by the manufacturer and approved by the institution physicist, commissioning should be the responsibility of an institution's qualified medical physicist.

As with acceptance testing, the details of commissioning for an MRgFUS unit may vary with manufacturer. Many of the commissioning tests will likely be similar to those for acceptance testing. However rather than simply demonstrating that the system meets its stated specifications, the commissioning tests are performed in order to determine the baseline performance of the system. As such, the level of attention and detail required for commissioning may be greater than that required simply to prove that a device meets its contractual requirements during acceptance testing.

6.4 Daily quality assurance testing

Daily quality assurance (DQA) testing of MRgFUS involves systematic checks and monitoring of selected parameters to determine compliance within acceptable limits before clinical use for a particular patient (or group of patients on a particular day). The purpose of such checks and monitoring is to confirm system safety and to detect changes in system performance before they can adversely affect positioning and heat delivery during therapy. Where a system is not used on a daily basis, the system's DQA procedures should be undertaken within the 24 hours before each patient treatment. Additional DQA at least 7 days prior to a treatment would allow any malfunction to be rectified without requiring a scheduling delay for the patient. While many methods for the calibration and characterization of ultrasound equipment are available (124-126) and QA programs for MRI are well established (127,128), there are few guidelines as to what constitutes an acceptable DQA protocol for MRgFUS.

DQA procedures focus on simple and reliable measurements, achievable in a clinical setting, that are sufficient to ensure system stability for the whole MRgFUS therapy device, including imaging guidance, power output, and targeting accuracy. Detection of problems that could lead to danger to the patient or the treatment team is of primary importance. Due to heavy demands on MRI time, it would be desirable to keep the duration of DQA testing to a minimum. While the more extensive pre-shipment or acceptance testing methods may include measurements such as acoustic output with a radiation force balance, or mapping the pressure or intensity distribution using a hydrophone, temperature probe, or optical system, their regular performance may not be practical. Some are impractical at high acoustic power levels or inside the magnet bore and do not characterize the imaging quality or transducer positioning system. There are certain checks, tests, and measurements, however, that can be performed daily, or prior to therapy, to verify the safety, functionality, and performance of the system.

The MRgFUS DQA procedure should ideally be executed by the site technologist or physicist before the first patient of the day. Specific checks will vary by machine, but should include visual checks for fluid leaks, cracks, or other defects in the ultrasound window, as well as verification that cables, hoses, and connectors are undamaged. The DQA procedure should also include routine checks for the MR imaging coil, transducer positioning system, operator safety device, as well as the patient emergency safety device functionality.

A key component of any DQA procedure for MRgFUS would include performing test sonications

into a tissue-mimicking phantom that is acoustically coupled to the therapy tabletop using degassed water to ensure the system works in an end-to-end fashion within acceptable clinical limits. In normal use, the MRgFUS system is centered in the magnet bore. Any errors in ultrasound output, transducer positioning, and/or table positioning can result in shifts in both the magnitude and location of the intended temperature elevation, relative to the delivered heating in the phantom. Possible deviations are investigated by sonication of a tissue-mimicking phantom while monitoring heating with MRTI. Sonication into a phantom while collecting real-time temperature maps allows quick performance assessment of a clinical MRgFUS device: the acoustic output is represented by the temperature rise curve and the maximum temperature achieved, the targeting accuracy, and the size and geometry of the heating volume. An example of this type of testing is seen in **Figure 8**. The results are used to confirm the functionality and performance of the system. In addition, the history of recorded results enables the tracking of deviations, or of drift in system performance (129).

Upon initiating the DQA procedure, a number of sonications to multiple locations within the phantom are sequentially performed, followed by an analysis (sometimes automated by vendor software) of the results. In many cases the vendor will provide recommended pass/fail criteria. This task group recommends that in no case should the clinic adopt pass/fail criteria that is less stringent than the vendor's criteria without detailed justification.

DQA for existing MRgFUS devices commonly assess parameters such as the following:

- Shape, size, and position of the tissue-mimicking phantom as seen on MRI
- Image signal-to-noise ratio (SNR)
- Cross-sectional dimensions and shape of the heating pattern
- Maximum temperature elevation
- Rate of temperature increase
- Spatial targeting accuracy

In an ideal situation, all of these parameters should remain nearly constant from day to day. While some day-to-day variations in the aforementioned parameters should be expected, the results should be within acceptable, pre-defined limits. For example, the maximum temperature elevation should be within a few degrees of the nominal value. Similarly, the spatial targeting accuracy should be on the order of 2 mm.

The DQA procedure provides a rapid assessment of basic system functionality. If the QA fails, however, in some cases it may be difficult to differentiate between issues with the host MRI system, the tissue-mimicking phantom or its setup, and the MRgFUS system itself. For example, if the DQA procedure fails due to an insufficient temperature increase, this may be due to inadequate acoustic coupling between the tabletop and phantom, deteriorated or damaged phantom, or reduced acoustic output of the MRgFUS system. In these cases, repeating the DQA test or performing more substantial testing may be needed to locate the primary issue. If repeating the DQA test does not help, or if the test repeatedly fails, the service support of the vendor should be contacted.

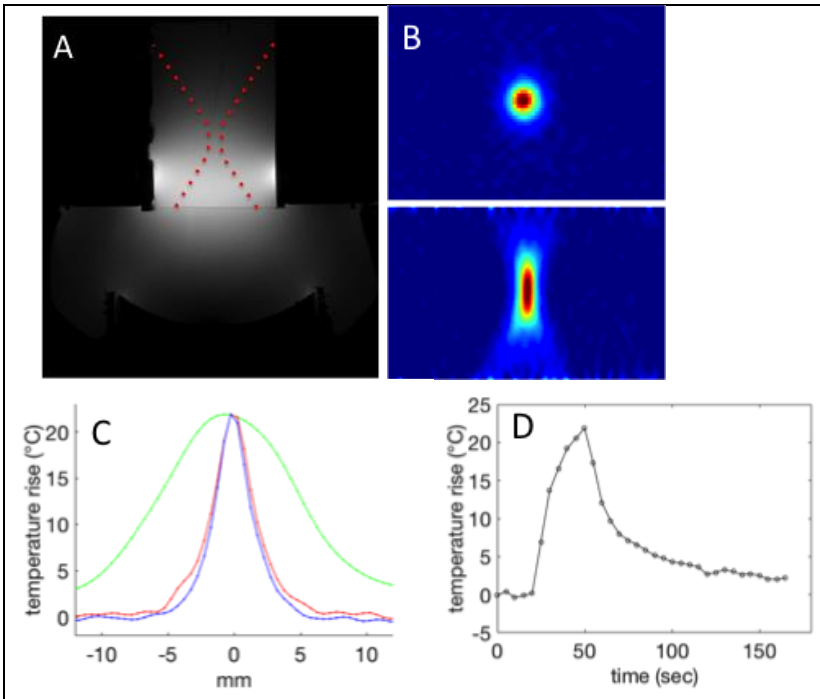

Figure 8: Example images of a DQA procedure. (A) T1w axial image showing the transducer, QA phantom and overlaid expected acoustic propagation path. (B) Spatial temperature maps of transverse (top) and longitudinal (bottom) orientations of the ultrasound beam. (C) Line plots of the ultrasound beam showing the size of the ultrasound beam pattern for longitudinal (green) and transverse (red and blue) directions. (D) Temperature versus time in maximum heating voxel.

6.5 Periodic testing

DQA procedures are basic by design, and are not intended to fully capture deviations in system performance. MRgFUS centers should also create a formal program of periodic testing that can compare system performance against the baseline obtained during commissioning as a way of detecting changes in the system over time. Periodic testing is commonly a spot check of commissioning results. The specific checks to be performed should ideally be informed as part of the risk-based analysis described in §6.2 as well as by accumulated clinical experience and experience with equipment failures. These tests may vary by equipment, and different tests may be performed at different time intervals. However the program should be formally written so it is simple to understand and rigorously followed. A partial list of areas the task group members have found important to check include the following (which are not meant to be exhaustive):

It is recommended to perform regular checks on the degassing system in order to ensure the quality of the acoustic coupling fluid. The formation of bubbles in the coupling fluid between the transducer and the skin surface may disturb the beam focusing and may lead to increased local heating if they are in close proximity to the skin itself. For systems in which the transducer is immersed in oil with a membrane interface to the patient skin there is unlikely to be a problem if all seals are unbroken. Where water is used, the oxygen content can be checked using a dissolved oxygen meter if there is user access to this compartment. An oxygen content level of $\leq$ 3 mg/L is usually considered to be acceptable. Where skin/membrane coupling is achieved using degassed water from an external degassing system, the oxygen content resulting from the

standard degassing protocol used before a patient treatment should be checked after every 20 patients or 6 months.

Where a fixed membrane forms an integral part of the transducer assembly, the membrane integrity should be checked after every 20 patients or 6 months. The table-top cover should be removed and the system inspected for leaks at this time. It is also important to check the table position and its homing ability relative to the magnet bore at the same intervals (see §6.3). The position of the transducer in the table, its movement capability (see §6.3) and the functioning of the patient emergency stop button should also be checked at these times.

The magnetic field and baseline temperature stability should be checked every 6 months using the methods used at acceptance (see §6.3). It should be ascertained that all elements of the MRI RF imaging coil are fully functioning. This should ideally be performed after each cohort of 20 patients. One method of doing this is to use an appropriate phantom, and to assess imaging from each element individually (130).

Although many systems indicate the status of transducer elements during the DQA tests, it is important to do a more thorough survey after every 100 treatments or 1 year. Associated with this should be a check of the transducer's electro-acoustic efficiency. This is most easily carried out using a measurement of acoustic power through radiation force balance testing.

Table 3 summarizes a suggested set of tests and frequencies required to maintain safety in an MRgFUS program with currently available equipment. As MRgFUS technology is continually evolving, this table should be viewed as a guide and not as a sufficient, comprehensive list.

Table 3: Recommended MRgFUS testing plan. The frequency recommendation should be implemented for whichever instance occurs first.

Test description	Measured parameter	Testing subset	Frequency
Transducer focusing capability	FWHM of beam	Acceptance, Commissioning, DQA	Either daily or before every patient
Transducer steering	Distance of beam steering	Acceptance, Commissioning, DQA	Either daily or before every patient
Imaging SNR	Comparison to baseline*	Acceptance, Commissioning, DQA	Either daily or before every patient
Safety interlock evaluation	Functionality	Acceptance, Commissioning, DQA	Either daily or before every patient
Visual check of the equipment for damage	Comparison to baseline*	Acceptance, Commissioning, DQA	Either daily or before every patient
Coupling membrane integrity inspection	Comparison to baseline*	Acceptance, Commissioning, DQA	Either daily or before every patient
Motor system evaluation	Comparison to baseline*	Acceptance, Commissioning, Periodic	Every 20 patients or 6 months
Table positioning and homing capability	Comparison to baseline*	Acceptance, Commissioning, Periodic	Every 20 patients or 6 months
MR temperature imaging accuracy	Comparison to invasive fiberoptic probe	Acceptance, Commissioning, Periodic	Every 20 patients or 6 months
Planning/delivery software function evaluation	Comparison to baseline*	Acceptance, Commissioning, Periodic	Every 20 patients or 6 months
Cavitation detection	Frequency spectrum	Acceptance,	Every 20 patients or

		Commissioning, Periodic	6 months
Degassing system	Oxygen content (ppm)	Acceptance, Commissioning, Periodic	Every 20 patients or 6 months
Acoustic output (radiation force balance)	Transducer output (in W)	Acceptance, Commissioning, Periodic	Every 100 patients or 1 year
Ultrasound beam characterization (hydrophone)	FWHM, I_{SPPA}	Acceptance, Commissioning, Periodic	Every 100 patients or 1 year

Baseline values obtained during commissioning testing

6.6 Key points and best practice recommendations

1. **Pre-shipment testing** performed by a manufacturer should ideally be reported to the customer institution before shipment.
2. **Formal risk analysis** should be conducted to identify and prioritize technical and clinical risk so they may be mitigated. The outcome of the formal risk analysis should be used to create formal QA procedures, frequencies, and tolerances.
3. **Periodic review of the risk analysis** should be performed to ensure appropriate QA frequencies and QA pass criteria are databased.
4. An **acceptance test** of an MRgFUS system should be conducted before final acceptance of the equipment from the manufacturer to ensure the system meets its contractual specifications. The acceptance tests are commonly performed by the manufacturer with participation and sign-off by the site technologist or physicist.
5. A set of **commissioning tests** with all required MRgFUS treatment equipment should be conducted before first clinical use of the system. This should result in a baseline characterization of system performance. The institution's qualified medical physicist should perform these tests.
6. A formal **DQA program** is critical to ensure the MRgFUS system is operating within expected limits before treating a patient or group of patients.

7: Responsibilities and training requirements of medical physicists for MRgFUS

MRgFUS procedures encompass a broad range of indications that span a large number of treatment sites. While the overall clinical oversight and decision-making process is the responsibility of the supervising physician, most MRgFUS procedures will likely be multidisciplinary in nature. The specific personnel requirements for MRgFUS will vary considerably with the specific indication and technique. Physicians involved in various procedures may include subspecialties such as oncology, interventional radiology and surgery. There may also be varying requirements for essential support staff including technicians, nurses, anesthesiologists and physicists. In all cases these essential team members require a proper level of training in order to ensure each team member can safely perform the required responsibility of their role.

Regardless of indication, MRgFUS procedures are comprised of a complicated set of techniques that are critically dependent on advanced, hybrid technology. This makes it imperative that the treatment team includes one or more team members with a technical background appropriate for ensuring the quality and safety of the treatment delivery. Medical physicists are in many cases an obvious choice to fill this role as they have direct experience in the therapeutic delivery of directed energy therapies and often have technical experience in imaging-centric technology.

7.1 Responsibilities of a qualified medical physicist for MRgFUS

While the details may vary by procedure, the responsibilities of an MRgFUS-trained medical physicist include:

1. The end-to-end technical performance of the MRgFUS system, including all imaging, localization, immobilization, treatment planning, and treatment delivery components.
2. The technical acceptance and initial commissioning of the MRgFUS system. The medical physicist must oversee the end-to-end technical operation of the MRgFUS system, work with the manufacturer(s) to complete contractual acceptance procedures, and create a baseline characterization of the system as part of system commissioning.
3. Evaluating the clinical workflow of the MRgFUS procedure for risk to the patient and developing strategies to mitigate this risk (120). This will include developing procedures for assuring the ability of the MRgFUS system to deliver a desired treatment as well as basic operational and safety QA procedures (§6).
4. Assisting in developing emergency response procedures in the setting of an unplanned technical or clinical event.

It may be that in some centers the complete set of required skills does not reside in a single individual. In this instance, it may be preferable for a team of physicists to jointly fulfill the responsibilities (for instance, a trained MR physicist and a trained therapy physicist with ultrasound and bioheat transfer experience (131)).

7.2 Recommended training guidelines

Before participating in an MRgFUS procedure it is critical that all team members are thoroughly trained, both on the technical use of the equipment and on the specific clinical procedures. A critical aspect of training for any procedure is support from the administration of an institution, which ultimately has the responsibility of formally credentialing team members to participate in an MRgFUS program. This task group recommends that any institution wishing to start an MRgFUS program create formal procedures for training and credentialing personnel who will participate in procedures. While no formal board certification currently exists for MRgFUS procedures, this report recommends the following qualification guidelines for a medical physicist participating in MRgFUS procedures (131):

1. The medical physicist should have an understanding of thermal dosimetry, MRI physics and therapeutic ultrasound with the knowledge of how these technologies interact during an MRgFUS procedure.
2. The medical physicist should receive vendor-specific training on the equipment to be used and for the specified indication. This training may be accomplished through a hands-on training program provided by the vendor (on-site or off-site) or by medical physicists already qualified for the specific equipment and indication.
3. Training should include a review of a formal risk analysis of the clinical procedure, hands-on instruction on intended treatment workflow, device operation, treatment planning/console operation, general safety procedures, MR-specific safety procedures, emergency procedures, and procedures for involving vendor service when appropriate.
4. If training is for an indication not currently offered, the vendor training program should include supervision of some agreed-upon number of cases (this task-group recommends a minimum of 3 cases) or the medical physicist should visit an institution currently offering the procedure and should observe some number of cases.
5. Whenever possible, the outcomes of peer-reviewed studies, and especially prospective clinical trials, should be used to guide clinical procedures. If the procedure

represents a new MRgFUS technique, then the procedure should be performed only after review and approval by the local institutional review board (IRB).

7.3 Ongoing training

Training materials should be reviewed on at least an annual basis by the treatment team. Changes in training materials should incorporate lessons learned by the treatment team, technical problems encountered, clinical workflow problems, near misses, and similar issues. Training materials should also be reviewed and updated after treatment machine upgrades.

All treatment team members should undergo refresher training annually or whenever significant changes to the training materials have been made. Individuals who fail to complete refresher training should be prevented from participating in procedures until their training can be brought up to date.

8: Regulatory Considerations

Since institutions with regulatory-approved MRgFUS systems may be interested in performing off-label clinical trials, this section details the requirements to obtain approval to use the approved device for investigational off-label use.

8.1. Regulatory Pathway for Clinical Trials to Evaluate Medical Devices

8.1.1 Investigational Device (IDE) Applications: The Center for Devices and Radiological Health (CDRH) in the Food and Drug Administration (FDA) Office of Medical Products and Tobacco is responsible for regulation of medical devices sold in the United States. As part of these responsibilities, CDRH reviews submissions for: 1) clinical trials to evaluate medical devices and 2) approval or clearance to market medical devices. This section will concentrate on the first type of submission because it may be of greater interest to medical physicists involved in clinical evaluation of MRgFUS devices. However, the preclinical characterization for MRgFUS devices (§8.1.2) would be similar for both types of submissions. A complete description of the formats, required elements, and processing of regulatory submissions to CDRH would require more space than is allowed in this Task Group Report. However, a brief summary of important concepts relevant to MRgFUS device regulation follows.

Clinical evaluation of the safety and effectiveness of medical devices falls under the Investigational Device Exemption regulations (21 CFR Part 812). These regulations require the submission of an IDE application to FDA prior to conducting a study on a *significant risk device*, where a significant risk device is one that presents a potential for serious risk to the health, safety, or welfare of a subject. The FDA considers many MRgFUS studies to be significant risk, requiring submission of an IDE application to FDA, unless exempt. Once an IDE application is approved by FDA, it must also be approved by the IRB(s) at the institution(s) where the study will be conducted before the study can begin.

A physician may use a medical device for an indication not in the approved labeling when the intent is treatment of a patient within a given practitioner-patient relationship. However, the physician has responsibility to base its use on sound medical evidence and to maintain records of the product's use and effects. Such "off-label" use does not require an IDE submission to FDA. The IRB for the institution where the device would be used may require review or oversight of off-label use, depending on institutional policies. The requirement for an IDE application depends on whether the off-label use is in the context of clinical practice or a

planned investigation. Off-label use to treat a particular patient in the best interest of the patient according to the physician's medical judgment is "practice of medicine," while using the device in a clinical investigation to *study* an off-label use may require an IDE, depending on the risk of the investigation.

An IDE application contains the following: 1) name and address of sponsor, 2) a report of prior investigation of the device, 3) an investigational plan, 4) a description of manufacture, processing, packing, storage, etc. of the device, 5) the agreement to be signed by investigators prior to their participation and a list of all investigators, 6) certification that all investigators will have signed the agreement prior to participating in the study, 7) information regarding all IRBs that have been or will be asked to review the protocol, 8) information regarding institutions where the investigation may be conducted, 9) amount (if any) charged for the device and an explanation of why sale does not constitute commercialization, 10) information regarding an environmental assessment, 11) device labeling information, 12) all informed consent materials and related information to be provided to subjects, and 13) any additional relevant information that the FDA requests in order to perform a complete review. Detailed requirements for the contents of the IDE application can be found in 21 CFR 812.20.

An IDE application may be approved, approved with conditions, or disapproved. If the IDE application is approved or approved with conditions, the study may begin after it is reviewed and approved by the IRB(s). If it is disapproved, the study may not begin until the sponsor responds to outstanding deficiencies and obtains approval. If the FDA does not inform the sponsor of one of these determinations within 30 days of receipt, then the IDE application is deemed approved.

Prior to submission of an IDE application, sponsors may contact the FDA to obtain further guidance through the pre-submission process (http://www.fda.gov/downloads/MedicalDevices/DeviceRegulationandGuidance/GuidanceDocuments/UCM311176.pdf).

Some key requirements in the IDE regulations are that: 1) investigational devices bear specific labeling indicating investigational use, 2) investigational devices are distributed only to qualified investigators, 3) informed consent is obtained from subjects participating in the study, 4) investigations are monitored to protect human subjects and assure compliance with approved protocols, 5) investigational devices are not commercialized or promoted, and 6) sponsors and investigators maintain specified records and provide appropriate reports.

More information regarding IDE regulations may be found at http://www.fda.gov/MedicalDevices/DeviceRegulationandGuidance/HowtoMarketYourDevice/InvestigationalDeviceExemptionIDE/default.htm.

8.1.2. Preclinical Testing for IDE Applications: The FDA may disapprove an IDE application for lack of compliance with IDE regulations, false information, inadequate response to FDA requests for additional information, inadequate informed consent, inadequate investigational plan, inadequate manufacturing, or inadequate monitoring. In addition, the FDA may disapprove an IDE application if the FDA finds that there is reason to believe that: 1) the risks to the human subjects are not outweighed by the anticipated benefits to the subjects or the importance of the knowledge to be gained, 2) the investigation as proposed is scientifically unsound, or 3) the device as used is ineffective. See 21 CFR 812.30(b) for more detail regarding the grounds for disapproval. In the case of MRgFUS devices, preclinical testing, as described below, can be helpful to address concerns related to risk/benefit, scientific soundness, and device effectiveness. In the case of investigation of a legally-marketed device

for a new indication, some of the following tests may have already been performed in order to obtain original FDA approval or clearance. However, depending on the extent of the modification or the change in intended use, previous tests may have diminished relevance and may need to be repeated under conditions more appropriate to the IDE application.

Due to the diversity in MRgFUS technological approaches and indications for use, it would be difficult to prescribe a specific procedure for testing to support all IDE applications. The following offers general considerations for characterization of MRgFUS system performance. This extends a basic framework for FDA regulation of HIFU (132), accounting for recent technological developments, progress in international standards development, and accumulated FDA experience with submissions for MRgFUS devices.

FDA submissions may be supported by conformance with standards published by professional organizations (see **Table 4**). Specifications that describe MRgFUS system performance include center frequency, peak rarefactional pressure, peak compressional pressure, acoustic intensity, acoustic power, duty cycle, and pulse duration.

Table 4: International Electrotechnical Commission (IEC) documents relevant to MRgFUS devices. (TS: Technical Specification, TR: Technical Report.)

Title	Number	Status	Recognized by FDA
Ultrasonics – Power measurement – High intensity therapeutic ultrasound (HITU) transducers and systems	IEC 62555	Published Ed 1.0, 2013	yes
Ultrasonics – Field characterization – Specification and measurement of field parameters for high intensity therapeutic ultrasound (HITU) transducers and systems	IEC/TS 62556	Published Ed. 1.0, 2014	
Medical electrical equipment –Part 2-62: Particular requirements for the basic safety and essential performance of high intensity therapeutic ultrasound (HITU) equipment	IEC 60601-2-62	Published Ed. 1.0, 2013	yes
Requirements for measurement standards for high intensity therapeutic ultrasound (HITU) devices	IEC/TR 62649	Published Ed. 1.0, 2010	
Measurement of ultrasound field parameters at high pressure therapeutic levels in water		Work in progress	
Ultrasonics - Field Characterization - measurement-based simulation in water and other media		Work in progress	

8.2 Technical information to support submissions to FDA

Characterization of free-field ultrasonic power and focusing: Ultrasound power output is often measured with a radiation force balance (37). An ultrasound wave may be directed toward a target that rests in a balance, which measures radiation force. In order to reduce problems associated with excessive target heating, measurements may be performed in burst mode and then extrapolated to continuous wave values (133). Measurements may become progressively less accurate as the ultrasound wave deviates from a plane wave, but correction factors may be applied to mitigate this problem (134). Another approach measures the change in buoyancy caused by thermal expansion of castor oil inside a target suspended in a water bath. The change in volume is proportional to the incident energy (135). Ultrasound power may

also be measured using the pyroelectric effect when an ultrasound wave is incident upon a thin piezoelectric polymer (polyvinylidene fluoride or PVDF) membrane bonded to a highly absorbing backing layer (36). The relative merits of different approaches have been analyzed in the context of focused ultrasound system quality assurance (136).

Hydrophones may be used to map the axial and lateral extent of the pressure fields in the focal zone. Special hydrophones have been designed to reduce the likelihood of damage or inaccurate measurements due to cavitation that can occur at focused ultrasound levels of intensity. These include membrane (137,138), needle (139), and fiber optic (140-142) designs. Hydrophone frequency-dependent sensitivity is often not uniform across the full spectra of focused ultrasound signals (which are very broadband due to the presence of many harmonics) and therefore sensitivity deconvolution may be required for accurate pressure measurements (143-147). Even with robust hydrophones, formidable challenges remain for making consistent, direct measurements of focused ultrasound pressures because of high intensity values, potential presence of shock fronts, challenges in positioning, and possibility of cavitation (148).

Because of practical difficulties associated with direct hydrophone measurements of focused ultrasound pressures, methods based on a combination of hydrophone measurements and computational modeling have been proposed. First, the pressure field of a source transducer is measured with a hydrophone under conditions of low-amplitude linear propagation. These measurements may be performed in the focal region along the axial dimension (and possibly the transverse dimension also) (149,150) or throughout a planar region intercepting the entire ultrasound beam (151,152). Then, linear propagation modeling is used to estimate the effective pressure distribution across the source transducer surface (153). Finally, computational modeling based on the Khokhlov–Zabolotskaya–Kuznetsov (KZK) or Westervelt equation is used to predict the pressure distribution under clinical nonlinear conditions. Other potential methods for characterization of focused ultrasound pressure fields involve optical methods (including Schlieren) (125,154,155) and streaming (156).

Demonstration of effective lesion formation: Experiments to demonstrate effective lesion formation may be performed in tissue-mimicking materials (TMMs), *ex vivo* tissue, *in vivo* tissue, or some combination. TMM tests are useful because they are relatively simple, inexpensive, and reproducible. In addition, they can yield temperature vs. time profiles similar to those measured in *ex vivo* tissue (157). However, the value of MRgFUS experiments in TMMs and *ex vivo* tissue may be limited if they do not match *in vivo* conditions, particularly perfusion. Many formulas for TMMs have been proposed (158-168). The choice of TMM will depend on the application.

Time-dependent temperature profiles may be measured using thermocouples embedded into TMM or tissue. Investigators should understand potential errors due to viscous heating from relative motion between the thermocouple and the surrounding medium (36,169), which may be mitigated by using extrapolation from measurements performed during the cooling period that begins immediately following the end of sonication (157,170). Investigators must also be aware of potential effects due to bubbles (*e.g.*, from cavitation or boiling), which can produce enhanced heating and/or shielding (157,158,171,172). Thin-film thermocouples may be less susceptible to viscous heating artifacts than fine-wire thermocouples (36). Thermocouples may be chosen with dimensions that are small compared to a wavelength in order to minimize distortion of the ultrasound field (173,174).

Computational modeling can complement experimental measurements for characterization of MRgFUS device performance. Modeling of nonlinear propagation may be based on the KZK or

Westervelt equation. Thermal analysis based on the bio-heat equation may be used to predict thermal dose contours (132). A free, downloadable software package called "HIFU Simulator" on the MathWorks website (Natick, MA) solves the KZK equation for the pressure distribution of an axisymmetric focused ultrasound transducer and provides accompanying thermal analysis (175). It is important to account for the effects of blood flow, which can have a significant effect on heating patterns (176-178).

Demonstration of accurate targeting and monitoring: MRgFUS device characterization may include an analysis of co-registration of planned vs. actual treatment zones (*i.e.*, targeting accuracy) and volumes. Treatment effectiveness may be supported by histopathological confirmation of the desired result at the cellular level (*e.g.*, coagulative necrosis) as well as images of treatment regions. The methods of thermal measurements, TMMs, and computational modeling discussed in the previous section may also be applied to demonstration of accurate targeting and monitoring.

MRgFUS device characterization may include an analysis of the effects of a variety of tissue types within or near the intended treatment volume. For example, if tissues that contain gas (*e.g.*, lungs and bowel) lie near the treatment volume, the effects of scattering from soft tissue/gas interfaces may affect MRgFUS device performance (136). Some tissues such as nerve tissue may be particularly sensitive to MRgFUS. Enhanced heating may occur near bone surfaces due to the relatively high absorption coefficient of bone (179-181). In order to ensure safety, the maximum temperature rise outside the intended treatment volume is of interest. Histology may be used to support safety of non-targeted tissue. Changes in beam structure due to temperature-dependent changes in tissue properties (especially speed of sound) can have noticeable effects on treatment zone location and size. If the MRgFUS device induces cavitation in tissues, then documentation of effective cavitation detection is an essential component of the device characterization.

The nature of clinical testing will depend on the indications for use. The safety and effectiveness of a particular MRgFUS device may sometimes be evaluated in the context of alternative therapies (*e.g.,* surgery, cryotherapy, radiofrequency ablation). Statistical methodology, including hypothesis testing and sample size justification, is always an important component of clinical testing.

8.3 Key points and best practice recommendations

1. MRgFUS devices are usually considered to be **significant risk devices** and therefore require approval of an Investigational Device Application (IDE) by the FDA before use in an investigational study.
2. **Complete characterization of an MRgFUS device** includes characterization of free-field ultrasonic power and focusing, demonstration of effective lesion formation, and demonstration of accurate targeting and monitoring.

9: Conclusions and recommendations

Magnetic resonance-guided focused ultrasound is a completely non-invasive technology that has been FDA approved to treat several diseases. While several specialized systems are approved and the number of commercial options continue to expand, this report describes and recommends best practices only for the clinical external body MRgFUS systems.

This hybrid technology requires medical physicists and other qualified personnel to be well-versed in multiple technologies including therapeutic ultrasound, thermal dosimetry and

magnetic resonance imaging. While current practices are well established among individual vendors, it is the job of the MRgFUS physicist to be able to identify potential sources of uncertainty in these procedures and recommend and manage the quality assurance programs required to adequately manage those uncertainties. This report has provided key points and best practice recommendations that will allow the identification and management of the uncertainties that can potentially arise during MRgFUS body treatments, ultimately affecting the treatment outcome.

MRgFUS is a developing technology with opportunities for continuous progression and improvement. The MRgFUS medical physicist can not only play a critical role in initiating and maintaining MRgFUS clinical programs, but also can provide insights and innovations that will continue to advance this technology into broader use in healthcare.

DISCLAIMER: The mention of commercial products, their sources, or their use in connection with material reported herein is not to be construed as either an actual or implied endorsement of such products by the Department of Health and Human Services.

Disclosure Statement:

1. The members of Task Group-241: MRI- Guided Focused Ultrasound listed below attest that they have no potential Conflicts of Interest related to the subject matter of materials presented in this document.

Chris Diederich, Dennis Parker, Eduardo Moros, Gail ter Haar, Lili Chen, Keyvan Farahani, David Schlesinger, Stanley Benedict, Jason Stafford, Steffen Sammet, Allison Payne

2. The members of Task Group-241: MRI- Guided Focused Ultrasound listed below disclose the following potential Conflict(s) of Interest related to subject matter or materials presented in this document.

Rajiv Chopra, an employee of UT Southwestern Medical Center, is a co-founder of Profound Medical, the manufacturer of one of the body MRgFUS systems described in this report.
Keith Wear is an employee of the US Food and Drug Administration.
Chrit Moonen has research collaborations with Profound Medical, with Philips Healthcare, and with Celsion Corporation.
Nicolas Ellens is an employee of Acertara Acoustic Laboratories, LLC.
Ari Partanen is a consultant for Profound Medical Inc.
Pejman Ghanouni, Stanford University, is on the medical advisory boards of INSIGHTEC and SonALAsense.

References

1. Hynyen K, McDannold N. MRI guided and monitored focused ultrasound thermal ablation methods: a review of progress. Int J Hyperthermia. 2004;20(7):725-37.
2. Fry WJ, Fry FJ. Fundamental neurological research and human neurosurgery using intense ultrasound. IRE Trans Med Electron. 1960;ME-7:166-81.
3. Fry FJ, Johnson LK. Tumor irradiation with intense ultrasound. Ultrasound Med Biol. 1978;4(4):337-41. PubMed PMID: 753007.
4. Lynn JG, Zwemer RL, Chick AJ, Miller AE. A New Method for the Generation and Use of Focused Ultrasound in Experimental Biology. J Gen Physiol. 1942;26(2):179-93. Epub 1942/11/20. PubMed PMID: 19873337.
5. Cline HE, Schenck JF, Hynynen K, Watkins RD, Souza SP, Jolesz FA. MR-guided focused ultrasound surgery. J Comput Assist Tomogr. 1992;16(6):956-65. PubMed PMID: 1430448.
6. Cline HE, Hynynen K, Hardy CJ, Watkins RD, Schenck JF, Jolesz FA. MR temperature mapping of focused ultrasound surgery. Magn Reson Med. 1994;31(6):628-36. PubMed PMID: 8057815.
7. Ringold S. FDA approves ultrasound fibroid therapy. Jama. 2004;292(23):2826. doi: 10.1001/jama.292.23.2826. PubMed PMID: 15598901.
8. Hynynen K, Clement GT, McDannold N, Vykhodtseva NI, King R, White PJ, Vitekand S, Jolesz FA. 500-element ultrasound phased array system for noninvasive focal surgery of the brain: a preliminary rabbit study with ex vivo human skulls. Magn Reson Med. 2004;52:100-7.
9. Nau WH, Diederich CJ, Ross AB, Butts K, Rieke V, Bouley DM, Gill H, Daniel B, Sommer G. MRI-guided interstitial ultrasound thermal therapy of the prostate: a feasibility study in the canine model. Med Phys. 2005;32(3):733-43. PubMed PMID: 15839345.
10. Haar GT, Coussios C. High intensity focused ultrasound: physical principles and devices. Int J Hyperthermia. 2007;23(2):89-104. PubMed PMID: 17578335.
11. Foundation FU. 2017 State of the Field Report **https://d3nqfeqdtaoni.cloudfront.net/images/pdf/FUSF-SOF-2017-32-web_secured.pdf**: Focused Ultrasound Foundation; 2017 [cited 2017 Jun 21, 2017].
12. Cline HE, Hynynen K, Watkins RD, Adams WJ, Schenck JF, Ettinger RH, Freund WR, Vetro JP, Jolesz FA. Focused US system for MR imaging-guided tumor ablation. Radiology. 1995;194(3):731-7. PubMed PMID: 7862971.
13. Cline HE, Schenck JF, Watkins RD, Hynynen K, Jolesz FA. Magnetic resonance-guided thermal surgery. Magn Reson Med. 1993;30(1):98-106. PubMed PMID: 8371680.
14. Philips. Sonalleve MR-HIFU Therapy Platform: Koninklijke Philips N.V.; 2017 [cited 2017 July, 14 2017]. Available from: http://www.philips.co.uk/healthcare/product/HC781360/sonalleve-mrhifu-therapy-platform.
15. Insightec. Insightec Company website: NGSOFT; 2017 [cited 2017 July 14, 2017]. Available from: http://www.insightec.com.
16. Kohler MO, Mougenot C, Quesson B, Enholm J, Le Bail B, Laurent C, Moonen CT, Ehnholm GJ. Volumetric HIFU ablation under 3D guidance of rapid MRI thermometry. Med Phys. 2009;36(8):3521-35. Epub 2009/09/15. PubMed PMID: 19746786.
17. Tempany CM, McDannold NJ, Hynynen K, Jolesz FA. Focused ultrasound surgery in oncology: overview and principles. Radiology. 2011;259(1):39-56. Epub 2011/03/26. doi: 259/1/39 [pii] 10.1148/radiol.11100155. PubMed PMID: 21436096.
18. Hynynen K, Freund WR, Cline HE, Chung AH, Watkins RD, Vetro JP, Jolesz FA. A clinical, noninvasive, MR imaging-monitored ultrasound surgery method. Radiographics. 1996;16(1):185-95. PubMed PMID: 10946699.

19. Salomir R, Quesson B, de Zwart JA, Vimeux F, Moonen C, editors. MR guided focused ultrasound hyperthermia: B0 field dynamic perturbation due to a moving transducer. International Society of Magnetic Resonance in Medicine; 2000.
20. Enholm JK, Kohler MO, Quesson B, Mougenot C, Moonen CT, Sokka SD. Improved volumetric MR-HIFU ablation by robust binary feedback control. IEEE Trans Biomed Eng. 2010;57(1):103-13. doi: 10.1109/TBME.2009.2034636. PubMed PMID: 19846364.
21. Quinn SD, Vedelago J, Regan L, Gedroyc WM. Safety and treatment volumes achieved following new developments of the magnetic resonance-guided focused ultrasound system in the treatment of uterine fibroids: a cohort study. J Ther Ultrasound. 2013;1:20. doi: 10.1186/2050-5736-1-20. PubMed PMID: 25512863; PMCID: PMC4265952.
22. Bobkova S, Gavrilov L, Khokhlova V, Shaw A, Hand J. Focusing of high-intensity ultrasound through the rib cage using a therapeutic random phased array. Ultrasound Med Biol. 2010;36(6):888-906. doi: 10.1016/j.ultrasmedbio.2010.03.007. PubMed PMID: 20510186; PMCID: PMC2879431.
23. Payne A, Vyas U, Todd N, de Bever J, Christensen DA, Parker DL. The effect of electronically steering a phased array ultrasound transducer on near-field tissue heating. Med Phys. 2011;38(9):4971-81. doi: 10.1118/1.3618729. PubMed PMID: 21978041; PMCID: 3166338.
24. McDannold N, Jolesz FA, Hynynen K. Determination of the optimal delay between sonifications during focused ultrasound surery in rabbits by using MR imaging to monitor thermal build up in vivo. Radiology. 1999;211:419-26.
25. Ikink ME, van Breugel JM, Schubert G, Nijenhuis RJ, Bartels LW, Moonen CT, van den Bosch MA. Volumetric MR-Guided High-Intensity Focused Ultrasound with Direct Skin Cooling for the Treatment of Symptomatic Uterine Fibroids: Proof-of-Concept Study. Biomed Res Int. 2015;2015:684250. doi: 10.1155/2015/684250. PubMed PMID: 26413538; PMCID: PMC4568047.
26. Chopra R, Burtnyk M, Haider MA, Bronskill MJ. Method for MRI-guided conformal thermal therapy of prostate with planar transurethral ultrasound heating applicators. Phys Med Biol. 2005;50(21):4957-75. doi: 10.1088/0031-9155/50/21/001. PubMed PMID: 16237234.
27. Lindner U, Ghai S, Spensieri P, Hlasny E, Van Der Kwast TH, McCluskey SA, Haider MA, Kucharczyk W, Trachtenberg J. Focal magnetic resonance guided focused ultrasound for prostate cancer: Initial North American experience. Can Urol Assoc J. 2012;6(6):E283-6. doi: 10.5489/cuaj.12218. PubMed PMID: 23283106; PMCID: PMC3529739.
28. Zaher S, Gedroyc W, Lyons D, Regan L. A novel method to aid in the visualisation and treatment of uterine fibroids with MRgFUS in patients with abdominal scars. Eur J Radiol. 2010;76(2):269-73. doi: 10.1016/j.ejrad.2009.07.004. PubMed PMID: 19665856.
29. Huisman M, ter Haar G, Napoli A, Hananel A, Ghanouni P, Lovey G, Nijenhuis RJ, van den Bosch MA, Rieke V, Majumdar S, Marchetti L, Pfeffer RM, Hurwitz MD. International consensus on use of focused ultrasound for painful bone metastases: Current status and future directions. Int J Hyperthermia. 2015;31(3):251-9. doi: 10.3109/02656736.2014.995237. PubMed PMID: 25677840.
30. Bucknor MD, Rieke V. MRgFUS for desmoid tumors within the thigh: early clinical experiences. J Ther Ultrasound. 2017;5:4. doi: 10.1186/s40349-017-0081-3. PubMed PMID: 28174660; PMCID: PMC5290631.
31. Rieke V, Butts Pauly K. MR thermometry. J Magn Reson Imaging. 2008;27(2):376-90. doi: 10.1002/jmri.21265. PubMed PMID: 18219673; PMCID: 2780364.
32. Hynynen K, Pomeroy O, Smith DN, Huber PE, McDannold NJ, Kettenbach J, Baum J, Singer S, Jolesz FA. MR imaging-guided focused ultrasound surgery of fibroadenomas in the breast: a feasibility study. Radiology. 2001;219(1):176-85. PubMed PMID: 11274554.

33. Lenard ZM, McDannold NJ, Fennessy FM, Stewart EA, Jolesz FA, Hynynen K, Tempany CM. Uterine leiomyomas: MR imaging-guided focused ultrasound surgery--imaging predictors of success. Radiology. 2008;249(1):187-94. Epub 2008/08/13. doi: 2491071600 [pii] 10.1148/radiol.2491071600. PubMed PMID: 18695211.
34. ter Haar G, Shaw A, Pye S, Ward B, Bottomley F, Nolan R, Coady AM. Guidance on reporting ultrasound exposure conditions for bio-effects studies. Ultrasound Med Biol. 2011;37(2):177-83. doi: 10.1016/j.ultrasmedbio.2010.10.021. PubMed PMID: 21257086.
35. Commission IE. IEC/TS 62556, Surgical systems -- Specification and measurement of field parameters for High Intensity Therapeutic Ultrasound (HITU) transducers and systems. 2012.
36. Shaw A, Hodnett M. Calibration and measurement issues for therapeutic ultrasound. Ultrasonics. 2008;48(4):234-52. doi: 10.1016/j.ultras.2007.10.010. PubMed PMID: 18234261.
37. Maruvada S, Harris GR, Herman BA, King RL. Acoustic power calibration of high-intensity focused ultrasound transducers using a radiation force technique. J Acoust Soc Am. 2007;121(3):1434-9. PubMed PMID: 17407880.
38. Wear KA, Howard SM. Correction for Spatial Averaging Artifacts in Hydrophone Measurements of High-Intensity Therapeutic Ultrasound: An Inverse Filter Approach. IEEE Trans Ultrason Ferroelectr Freq Control. 2019;66(9):1453-64. doi: 10.1109/TUFFC.2019.2924351. PubMed PMID: 31247548; PMCID: PMC6936621.
39. Khokhlova VA, Bailey MR, Reed JA, Cunitz BW, Kaczkowski PJ, Crum LA. Effects of nonlinear propagation, cavitation, and boiling in lesion formation by high intensity focused ultrasound in a gel phantom. J Acoust Soc Am. 2006;119(3):1834-48. PubMed PMID: 16583923.
40. Hockham N, Coussios CC, Arora M. A real-time controller for sustaining thermally relevant acoustic cavitation during ultrasound therapy. IEEE Trans Ultrason Ferroelectr Freq Control. 2010;57(12):2685-94. doi: 10.1109/TUFFC.2010.1742. PubMed PMID: 21156364.
41. Desjouy C, Poizat A, Gilles B, Inserra C, Bera JC. Control of inertial acoustic cavitation in pulsed sonication using a real-time feedback loop system. J Acoust Soc Am. 2013;134(2):1640-6. doi: 10.1121/1.4812973. PubMed PMID: 23927204.
42. Damianou CA, Sanghvi NT, Fry FJ, Maass-Moreno R. Dependence of ultrasonic attenuation and absorption in dog soft tissues on temperature and thermal dose. J Acoust Soc Am. 1997;102:628-34.
43. Ghoshal G, Luchies AC, Blue JP, Oelze ML. Temperature dependent ultrasonic characterization of biological media. J Acoust Soc Am. 2011;130(4):2203-11. doi: 10.1121/1.3626162. PubMed PMID: 21973375; PMCID: PMC3206913.
44. Law WK, Frizzell LA, Dunn F. Comparison of thermodynamic and finite amplitude methods of B/A measurement in biological materials. J Acoust Soc Am. 1983;74:1295-7.
45. Gong X-F, Zhu Z-M, Shi T, Huang J-H. Determination of the acoustic nonlinearity parameter in biological media using FAIS and ITD methods. J Acoust Soc Am. 1989;25:831-8.
46. Zeqiri B, Cook A, Retat L, Civale J, ter Haar G. On measurement of the acoustic nonlinearity parameter using the finite amplitude insertion substitution (FAIS) technique. Metrologia. 2015;52:406-22.
47. Dillon CR, Payne A, Christensen DA, Roemer RB. The accuracy and precision of two non-invasive, magnetic resonance-guided focused ultrasound-based thermal diffusivity estimation methods. Int J Hyperthermia. 2014;30(6):362-71. doi: 10.3109/02656736.2014.945497. PubMed PMID: 25198092.
48. Carslaw HS, Jaeger JC. Conduction of Heat in Solids. 2nd ed: Oxford University Press; 1959.
49. Hasgall PA DGF, Baumgartner C, Neufeld E, Gosselin MC, Payne D, Klingenböck A, Kuster N. IT'IS Database for thermal and electromagnetic parameters of biological tissues 2015 [updated September 01st, 2015; cited 2016]; Version 3.0:[

50. Dillon C, Roemer R, Payne A. Magnetic resonance temperature imaging-based quantification of blood flow-related energy losses. NMR in biomedicine. 2015;28(7):840-51. doi: 10.1002/nbm.3318. PubMed PMID: 25973583; PMCID: 4510856.
51. Dragonu I, de Oliveira PL, Laurent C, Mougenot C, Grenier N, Moonen CT, Quesson B. Non-invasive determination of tissue thermal parameters from high intensity focused ultrasound treatment monitored by volumetric MRI thermometry. NMR in biomedicine. 2009;22(8):843-51. Epub 2009/06/30. doi: 10.1002/nbm.1397. PubMed PMID: 19562728.
52. Pennes HH. Analysis of tissue and arterial blood temperatures in the resting human forearm. J Appl Physiol. 1948;1(2):93-122. Epub 1948/08/01. PubMed PMID: 18887578.
53. Bhattacharya A, Mahajan RL. Temperature dependence of thermal conductivity of biological tissues. Physiol Meas. 2003;24(3):769-83. PubMed PMID: 14509313.
54. Song CW, Rhee JG, Levitt SH. Blood flow in normal tissues and tumors during hyperthermia. J Natl Cancer Inst. 1980;64(1):119-24. PubMed PMID: 6928036.
55. MacFall JR, Prescott DM, Charles HC, Samulski TV. 1H MRI phase thermometry in vivo in canine brain, muscle, and tumor tissue. Med Phys. 1996;23(10):1775-82. PubMed PMID: 8946373.
56. De Poorter J, De Wagter C, De Deene Y, Thomsen C. The proton resonance frequency shift method compared with molecular diffusion for quantitative measurement of two-dimensional time-dependent temperature distribution in a phantom. J Magn Reson, Series B. 1994;103:234-41.
57. De Poorter J. Noninvasive MRI thermometry with the proton resonance frequency method: study of susceptibility effects. Magn Reson Med. 1995;34(3):359-67. PubMed PMID: 7500875.
58. Todd N, Diakite M, Payne A, Parker DL. Hybrid proton resonance frequency/T1 technique for simultaneous temperature monitoring in adipose and aqueous tissues. Magn Reson Med. 2013;69(1):62-70. Epub 2012/03/07. doi: 10.1002/mrm.24228. PubMed PMID: 22392856.
59. Baron P, Deckers R, de Greef M, Merckel LG, Bakker CJ, Bouwman JG, Bleys RL, van den Bosch MA, Bartels LW. Correction of proton resonance frequency shift MR-thermometry errors caused by heat-induced magnetic susceptibility changes during high intensity focused ultrasound ablations in tissues containing fat. Magn Reson Med. 2014;72(6):1580-9. doi: 10.1002/mrm.25063. PubMed PMID: 24347129.
60. Baron P, Deckers R, Bouwman JG, Bakker CJ, de Greef M, Viergever MA, Moonen CT, Bartels LW. Influence of water and fat heterogeneity on fat-referenced MR thermometry. Magn Reson Med. 2015. doi: 10.1002/mrm.25727. PubMed PMID: 25940426.
61. Ozhinsky E, Kohi MP, Ghanouni P, Rieke V. T2-based temperature monitoring in abdominal fat during MR-guided focused ultrasound treatment of patients with uterine fibroids. J Ther Ultrasound. 2015;3:15. doi: 10.1186/s40349-015-0036-5. PubMed PMID: 26366288; PMCID: PMC4567827.
62. Delannoy J, Chen CN, Turner R, Levin RL, Le Bihan D. Noninvasive temperature imaging using diffusion MRI. Magn Reson Med. 1991;19(2):333-9. PubMed PMID: 1881323.
63. Denis de Senneville B, Quesson B, Moonen CT. Magnetic resonance temperature imaging. Int J Hyperthermia. 2005;21(6):515-31. doi: 10.1080/02656730500133785. PubMed PMID: 16147437.
64. Kuroda K. MR techniques for guiding high-intensity focused ultrasound (HIFU) treatments. J Magn Reson Imaging. 2017. doi: 10.1002/jmri.25770. PubMed PMID: 28580706.
65. Shaw A, ter Haar G, Haller J, Wilkens V. Towards a dosimetric framework for therapeutic ultrasound. Int J Hyperthermia. 2015;31(2):182-92. doi: 10.3109/02656736.2014.997311. PubMed PMID: 25774889.
66. Sapareto SA, Dewey WC. Thermal dose determination in cancer therapy. Int J Radiation Oncology Biol Phys. 1984;10:787-800.

67. Dewhirst MW, Viglianti BL, Lora-Michiels M, Hanson M, Hoopes PJ. Basic principles of thermal dosimetry and thermal thresholds for tissue damage from hyperthermia. Int J Hyperthermia. 2003;19(3):267-94.
68. Yarmolenko PS, Moon EJ, Landon C, Manzoor A, Hochman DW, Viglianti BL, Dewhirst MW. Thresholds for thermal damage to normal tissues: an update. Int J Hyperthermia. 2011;27(4):320-43. doi: 10.3109/02656736.2010.534527. PubMed PMID: 21591897; PMCID: PMC3609720.
69. Hindley J, Gedroyc WM, Regan L, Stewart E, Tempany C, Hynyen K, McDannold N, Inbar Y, Itzchak Y, Rabinovici J, Kim HS, Geschwind JF, Hesley G, Gostout B, Ehrenstein T, Hengst S, Sklair-Levy M, Shushan A, Jolesz F. MRI guidance of focused ultrasound therapy of uterine fibroids: early results. Ajr. 2004;183(6):1713-9. PubMed PMID: 15547216.
70. Stewart EA, Gedroyc WM, Tempany CM, Quade BJ, Inbar Y, Ehrenstein T, Shushan A, Hindley JT, Goldin RD, David M, Sklair M, Rabinovici J. Focused ultrasound treatment of uterine fibroid tumors: safety and feasibility of a noninvasive thermoablative technique. American journal of obstetrics and gynecology. 2003;189(1):48-54. PubMed PMID: 12861137.
71. Tempany CM, Stewart EA, McDannold N, Quade BJ, Jolesz FA, Hynynen K. MR imaging-guided focused ultrasound surgery of uterine leiomyomas: a feasibility study. Radiology. 2003;226(3):897-905. PubMed PMID: 12616023.
72. McDannold N, Tempany CM, Fennessy FM, So MJ, Rybicki FJ, Stewart EA, Jolesz FA, Hynynen K. Uterine leiomyomas: MR imaging-based thermometry and thermal dosimetry during focused ultrasound thermal ablation. Radiology. 2006;240(1):263-72. PubMed PMID: 16793983.
73. Hijnen NM, Elevelt A, Grull H. Stability and trapping of magnetic resonance imaging contrast agents during high-intensity focused ultrasound ablation therapy. Invest Radiol. 2013;48(7):517-24. doi: 10.1097/RLI.0b013e31829aae98. PubMed PMID: 23695082.
74. Hectors SJ, Jacobs I, Moonen CT, Strijkers GJ, Nicolay K. MRI methods for the evaluation of high intensity focused ultrasound tumor treatment: Current status and future needs. Magn Reson Med. 2016;75(1):302-17. doi: 10.1002/mrm.25758. PubMed PMID: 26096859.
75. Winter L, Oberacker E, Paul K, Ji Y, Oezerdem C, Ghadjar P, Thieme A, Budach V, Wust P, Niendorf T. Magnetic resonance thermometry: Methodology, pitfalls and practical solutions. Int J Hyperthermia. 2016;32(1):63-75. doi: 10.3109/02656736.2015.1108462. PubMed PMID: 26708630.
76. Wijlemans JW, Deckers R, van den Bosch MA, Seinstra BA, van Stralen M, van Diest PJ, Moonen CT, Bartels LW. Evolution of the ablation region after magnetic resonance-guided high-intensity focused ultrasound ablation in a Vx2 tumor model. Invest Radiol.48(6):381-6. Epub 2013/02/13. doi: 10.1097/RLI.0b013e3182820257. PubMed PMID: 23399810.
77. Burnet NG, Thomas SJ, Burton KE, Jefferies SJ. Defining the tumour and target volumes for radiotherapy. Cancer Imaging. 2004;4(2):153-61. doi: 10.1102/1470-7330.2004.0054. PubMed PMID: 18250025; PMCID: PMC1434601.
78. Clarke RL, Bush NL, Ter Haar GR. The changes in acoustic attenuation due to in vitro heating. Ultrasound Med Biol. 2003;29(1):127-35. PubMed PMID: 12604124.
79. McDannold N. Quantitative MRI-based temperature mapping based on the proton resonant frequency shift: review of validation studies. Int J Hyperthermia. 2005;21(6):533-46. PubMed PMID: 16147438.
80. Todd N, Vyas U, de Bever J, Payne A, Parker DL. The effects of spatial sampling choices on MR temperature measurements. Magn Reson Med. 2011;65(2):515-21. Epub 2010/10/01. doi: 10.1002/mrm.22636. PubMed PMID: 20882671.
81. El-Sharkawy AM, Schar M, Bottomley PA, Atalar E. Monitoring and correcting spatio-temporal variations of the MR scanner's static magnetic field. MAGMA. 2006;19(5):223-36. doi: 10.1007/s10334-006-0050-2. PubMed PMID: 17043837; PMCID: PMC1945237.

82. De Poorter J, De Wagter C, De Deene Y, Thomsen C, Stahlberg F, Achten E. Noninvasive MRI thermometry with the proton resonance frequency (PRF) method: in vivo results in human muscle. Magn Reson Med. 1995;33(1):74-81. PubMed PMID: 7891538.
83. Rieke V, Kinsey AM, Ross AB, Nau WH, Diederich CJ, Sommer G, Pauly KB. Referenceless MR thermometry for monitoring thermal ablation in the prostate. IEEE Trans Med Imaging. 2007;26(6):813-21. doi: 10.1109/TMI.2007.892647. PubMed PMID: 17679332; PMCID: PMC2780365.
84. Young IR, Hajnal JV, Roberts IG, Ling JX, Hill-Cottingham RJ, Oatridge A, Wilson JA. An evaluation of the effects of susceptibility changes on the water chemical shift method of temperature measurement in human peripheral muscle. Magn Reson Med. 1996;36(3):366-74. PubMed PMID: 8875406.
85. Gedroyc WM. New clinical applications of magnetic resonance-guided focused ultrasound. Top Magn Reson Imaging. 2006;17(3):189-94. doi: 10.1097/RMR.0b013e318038f782. PubMed PMID: 17414076.
86. Kopelman D, Inbar Y, Hanannel A, Freundlich D, Castel D, Perel A, Greenfeld A, Salamon T, Sareli M, Valeanu A, Papa M. Magnetic resonance-guided focused ultrasound surgery (MRgFUS): ablation of liver tissue in a porcine model. Eur J Radiol. 2006;59(2):157-62. PubMed PMID: 16725294.
87. Okada A, Murakami T, Mikami K, Onishi H, Tanigawa N, Marukawa T, Nakamura H. A case of hepatocellular carcinoma treated by MR-guided focused ultrasound ablation with respiratory gating. Magn Reson Med Sci. 2006;5(3):167-71. PubMed PMID: 17139143.
88. Wijlemans JW, de Greef M, Schubert G, Moonen CT, van den Bosch MA, Ries M. Intrapleural fluid infusion for MR-guided high-intensity focused ultrasound ablation in the liver dome. Acad Radiol. 2014;21(12):1597-602. doi: 10.1016/j.acra.2014.06.015. PubMed PMID: 25126972.
89. Auboiroux V, Petrusca L, Viallon M, Muller A, Terraz S, Breguet R, Montet X, Becker CD, Salomir R. Respiratory-gated MRgHIFU in upper abdomen using an MR-compatible in-bore digital camera. Biomed Res Int. 2014;2014:421726. doi: 10.1155/2014/421726. PubMed PMID: 24716196; PMCID: PMC3925565.
90. Holbrook AB, Ghanouni P, Santos JM, Dumoulin C, Medan Y, Pauly KB. Respiration based steering for high intensity focused ultrasound liver ablation. Magn Reson Med. 2014;71(2):797-806. doi: 10.1002/mrm.24695. PubMed PMID: 23460510; PMCID: PMC4040338.
91. de Zwart JA, Vimeux FC, Palussiere J, Salomir R, Quesson B, Delalande C, Moonen CT. On-line correction and visualization of motion during MRI-controlled hyperthermia. Magn Reson Med. 2001;45(1):128-37. PubMed PMID: 11146494.
92. de Senneville BD, Mougenot C, Moonen CT. Real-time adaptive methods for treatment of mobile organs by MRI-controlled high-intensity focused ultrasound. Magn Reson Med. 2007;57(2):319-30. PubMed PMID: 17260361.
93. Kohler MO, Denis de Senneville B, Quesson B, Moonen CT, Ries M. Spectrally selective pencil-beam navigator for motion compensation of MR-guided high-intensity focused ultrasound therapy of abdominal organs. Magn Reson Med. 2011;66(1):102-11. doi: 10.1002/mrm.22784. PubMed PMID: 21305602.
94. Stemkens B, Tijssen RH, de Senneville BD, Heerkens HD, van Vulpen M, Lagendijk JJ, van den Berg CA. Optimizing 4-dimensional magnetic resonance imaging data sampling for respiratory motion analysis of pancreatic tumors. Int J Radiat Oncol Biol Phys. 2015;91(3):571-8. doi: 10.1016/j.ijrobp.2014.10.050. PubMed PMID: 25596109.
95. Ries M, de Senneville BD, Roujol S, Berber Y, Quesson B, Moonen C. Real-time 3D target tracking in MRI guided focused ultrasound ablations in moving tissues. Magn Reson Med. 2010;64(6):1704-12. doi: 10.1002/mrm.22548. PubMed PMID: 20878763.

96. Arnold P, Preiswerk F, Fasel B, Salomir R, Scheffler K, Cattin PC. 3D organ motion prediction for MR-guided high intensity focused ultrasound. Med Image Comput Comput Assist Interv. 2011;14(Pt 2):623-30. PubMed PMID: 21995081.
97. Denis de Senneville B, El Hamidi A, Moonen C. A direct PCA-based approach for real-time description of physiological organ deformations. IEEE Trans Med Imaging. 2015;34(4):974-82. doi: 10.1109/TMI.2014.2371995. PubMed PMID: 25423649.
98. Pernot M, Aubry JF, Tanter M, Thomas JL, Fink M. High power transcranial beam steering for ultrasonic brain therapy. Phys Med Biol. 2003;48(16):2577-89. PubMed PMID: 12974575.
99. de Oliveira PL, de Senneville BD, Dragonu I, Moonen CT. Rapid motion correction in MR-guided high-intensity focused ultrasound heating using real-time ultrasound echo information. NMR in biomedicine. 2010;23(9):1103-8. doi: 10.1002/nbm.1526. PubMed PMID: 20669159.
100. Young IR, Hand JW, Oatridge A, Prior MV. Modeling and observation of temperature changes in vivo using MRI. Magn Reson Med. 1994;32(3):358-69. PubMed PMID: 7984068.
101. Vigen KK, Daniel BL, Pauly JM, Butts K. Triggered, navigated, multi-baseline method for proton resonance frequency temperature mapping with respiratory motion. Magn Reson Med. 2003;50(5):1003-10. doi: 10.1002/mrm.10608. PubMed PMID: 14587011.
102. Quesson B, Laurent C, Maclair G, de Senneville BD, Mougenot C, Ries M, Carteret T, Rullier A, Moonen CT. Real-time volumetric MRI thermometry of focused ultrasound ablation in vivo: a feasibility study in pig liver and kidney. NMR in biomedicine.24(2):145-53. Epub 2011/02/24. doi: 10.1002/nbm.1563. PubMed PMID: 21344531.
103. Rieke V, Vigen KK, Sommer FG, Daniel BL, Pauly JM, Butts K. Referenceless PRF shift thermometry. Magn Reson Med. 2004;51(6):1223-31.
104. Holbrook AB, Santos JM, Kaye E, Rieke V, Pauly KB. Real-time MR thermometry for monitoring HIFU ablations of the liver. Magn Reson Med. 2010;63(2):365-73. doi: 10.1002/mrm.22206. PubMed PMID: 19950255; PMCID: 3212435.
105. Grissom WA, Rieke V, Holbrook AB, Medan Y, Lustig M, Santos J, McConnell MV, Pauly KB. Hybrid referenceless and multibaseline subtraction MR thermometry for monitoring thermal therapies in moving organs. Med Phys. 2010;37(9):5014-26. PubMed PMID: 20964221; PMCID: 2945742.
106. McDannold N, Tempany C, Jolesz F, Hynynen K. Evaluation of referenceless thermometry in MRI-guided focused ultrasound surgery of uterine fibroids. J Magn Reson Imaging. 2008;28(4):1026-32. doi: 10.1002/jmri.21506. PubMed PMID: 18821603; PMCID: PMC2574694.
107. Salomir R, Viallon M, Kickhefel A, Roland J, Morel DR, Petrusca L, Auboiroux V, Goget T, Terraz S, Becker CD, Gross P. Reference-free PRFS MR-thermometry using near-harmonic 2-D reconstruction of the background phase. IEEE Trans Med Imaging. 2012;31(2):287-301. doi: 10.1109/TMI.2011.2168421. PubMed PMID: 21937345.
108. Miralbell R, Nouet P, Rouzaud M, Bardina A, Hejira N, Schneider D. Radiotherapy of bladder cancer: relevance of bladder volume changes in planning boost treatment. Int J Radiat Oncol Biol Phys. 1998;41(4):741-6. PubMed PMID: 9652833.
109. Langen KM, Willoughby TR, Meeks SL, Santhanam A, Cunningham A, Levine L, Kupelian PA. Observations on real-time prostate gland motion using electromagnetic tracking. Int J Radiat Oncol Biol Phys. 2008;71(4):1084-90. doi: 10.1016/j.ijrobp.2007.11.054. PubMed PMID: 18280057.
110. Smitsmans MH, Pos FJ, de Bois J, Heemsbergen WD, Sonke JJ, Lebesque JV, van Herk M. The influence of a dietary protocol on cone beam CT-guided radiotherapy for prostate cancer patients. Int J Radiat Oncol Biol Phys. 2008;71(4):1279-86. doi: 10.1016/j.ijrobp.2008.03.036. PubMed PMID: 18572088.

111. Emmott J, Sanghera B, Chambers J, Wong WL. The effects of N-butylscopolamine on bowel uptake: an 18F-FDG PET study. Nucl Med Commun. 2008;29(1):11-6. doi: 10.1097/MNM.0b013e3282f1d706. PubMed PMID: 18049092.
112. Verhey LJ. Immobilizing and Positioning Patients for Radiotherapy. Semin Radiat Oncol. 1995;5(2):100-14. doi: 10.1054/SRAO00500100. PubMed PMID: 10717133.
113. Zhang L, Chen WZ, Liu YJ, Hu X, Zhou K, Chen L, Peng S, Zhu H, Zou HL, Bai J, Wang ZB. Feasibility of magnetic resonance imaging-guided high intensity focused ultrasound therapy for ablating uterine fibroids in patients with bowel lies anterior to uterus. Eur J Radiol. 2010;73(2):396-403. doi: 10.1016/j.ejrad.2008.11.002. PubMed PMID: 19108974.
114. McDannold N, Hynynen K, J F. MRI monitoring of the thermal ablation of tissue: effects of long exposure times. Journal of Magnetic Resonance Imaging. 2001;13:421-7.
115. Todd N, Prakash J, Odeen H, de Bever J, Payne A, Yalavarthy P, Parker DL. Toward real-time availability of 3D temperature maps created with temporally constrained reconstruction. Magn Reson Med. 2014;71(4):1394-404. doi: 10.1002/mrm.24783. PubMed PMID: 23670981; PMCID: 3778054.
116. Roujol S, de Senneville BD, Hey S, Moonen C, Ries M. Robust adaptive extended Kalman filtering for real time MR-thermometry guided HIFU interventions. IEEE Trans Med Imaging. 2012;31(3):533-42. doi: 10.1109/TMI.2011.2171772. PubMed PMID: 21997254.
117. Denis de Senneville B, Roujol S, Hey S, Moonen C, Ries M. Extended Kalman filtering for continuous volumetric MR-temperature imaging. IEEE Trans Med Imaging. 2013;32(4):711-8. doi: 10.1109/TMI.2012.2234760. PubMed PMID: 23268383.
118. Bitton RR, Webb TD, Pauly KB, Ghanouni P. Improving thermal dose accuracy in magnetic resonance-guided focused ultrasound surgery: Long-term thermometry using a prior baseline as a reference. J Magn Reson Imaging. 2016;43(1):181-9. doi: 10.1002/jmri.24978. PubMed PMID: 26119129; PMCID: PMC4691444.
119. Administration USFaD. Quality System (QS) Regulation/Medical Device Good Manufacturing Practices 2016 [cited 2017]. Available from: https://www.fda.gov/MedicalDevices/DeviceRegulationandGuidance/PostmarketRequirements/QualitySystemsRegulations/default.htm.
120. Huq MS, Fraass BA, Dunscombe PB, Gibbons JP, Jr., Ibbott GS, Mundt AJ, Mutic S, Palta JR, Rath F, Thomadsen BR, Williamson JF, Yorke ED. The report of Task Group 100 of the AAPM: Application of risk analysis methods to radiation therapy quality management. Med Phys. 2016;43(7):4209. doi: 10.1118/1.4947547. PubMed PMID: 27370140; PMCID: PMC4985013.
121. Novak P, Moros EG, Straube WL, Myerson RJ. Treatment delivery software for a new clinical grade ultrasound system for thermoradiotherapy. Med Phys. 2005;32(11):3246-56. doi: 10.1118/1.2064848. PubMed PMID: 16372408.
122. Jackson E, Bronskill M, Drost D, Och J, Pooley R, Sobol W, Clarke GD. Acceptance testing and quality assurance procedures for magnetic resonance imaging facilities. College Park, MD: 2010.
123. Gorny KR, Hangiandreou NJ, Hesley GK, Gostout BS, McGee KP, Felmlee JP. MR guided focused ultrasound: technical acceptance measures for a clinical system. Phys Med Biol. 2006;51(12):3155-73. PubMed PMID: 16757869.
124. Wong GS, Wu L. High power ultrasound standard. J Acoust Soc Am. 2002;111(4):1791-9. PubMed PMID: 12002863.
125. Harris GR. Progress in medical ultrasound exposimetry. IEEE Trans Ultrason Ferroelectr Freq Control. 2005;52(5):717-36. PubMed PMID: 16048175.
126. Lewin PA, Barrie-Smith N, Ide M, Hynynen K, Macdonald M. Interlaboratory acoustic power measurement. J Ultrasound Med. 2003;22(2):207-13. PubMed PMID: 12562125.
127. Price RR, Axel L, Morgan T, Newman R, Perman W, Schneiders N, Selikson M, Wood M, Thomas SR. Quality assurance methods and phantoms for magnetic resonance imaging:

report of AAPM nuclear magnetic resonance Task Group No. 1. Med Phys. 1990;17(2):287-95. doi: 10.1118/1.596566. PubMed PMID: 2333055.
128. Lerski RA, de Certaines JD. Performance assessment and quality control in MRI by Eurospin test objects and protocols. Magn Reson Imaging. 1993;11(6):817-33. PubMed PMID: 8371637.
129. McDannold N, Hynynen K. Quality assurance and system stability of a clinical MRI-guided focused ultrasound system: four-year experience. Med Phys. 2006;33(11):4307-13. PubMed PMID: 17153409.
130. Radiology ACo, Medicine AAoPi. ACR-AAPM technical standard for diagnostic medical physics performance monitoring of magnetic resonance imaging (MRI). MRI Equipment2010.
131. Myerson RJ, Moros EG, Diederich CJ, Haemmerich D, Hurwitz MD, Hsu IC, McGough RJ, Nau WH, Straube WL, Turner PF, Vujaskovic Z, Stauffer PR. Components of a hyperthermia clinic: recommendations for staffing, equipment, and treatment monitoring. Int J Hyperthermia. 2014;30(1):1-5. doi: 10.3109/02656736.2013.861520. PubMed PMID: 24350642.
132. Harris GR. FDA regulation of clinical high intensity focused ultrasound (HIFU) devices. Conf Proc IEEE Eng Med Biol Soc. 2009;2009:145-8. doi: 10.1109/IEMBS.2009.5332444. PubMed PMID: 19963452.
133. Haller J, Wilkens V. Derivation of continuous wave mode output power from burst mode measurements in high-intensity ultrasound applications. J Acoust Soc Am. 2014;135(3):EL123-7. doi: 10.1121/1.4865268. PubMed PMID: 24606304.
134. Gelat P, Shaw A. Relationship between acoustic power and acoustic radiation force on absorbing and reflecting targets for spherically focusing radiators. Ultrasound Med Biol. 2015;41(3):832-44. doi: 10.1016/j.ultrasmedbio.2014.09.021. PubMed PMID: 25683223.
135. Shaw A. A buoyancy method for the measurement of total ultrasound power generated by HIFU transducers. Ultrasound Med Biol. 2008;34(8):1327-42. doi: 10.1016/j.ultrasmedbio.2008.01.008. PubMed PMID: 18471952.
136. Civale J, Rivens I, ter Haar G. Quality assurance for clinical high intensity focused ultrasound fields. Int J Hyperthermia. 2015;31(2):193-202. doi: 10.3109/02656736.2014.1002435. PubMed PMID: 25677839.
137. Bessonova OV, Wilkens V. Membrane hydrophone measurement and numerical simulation of HIFU fields up to developed shock regimes. IEEE Trans Ultrason Ferroelectr Freq Control. 2013;60(2):290-300. doi: 10.1109/TUFFC.2013.2565. PubMed PMID: 23357903.
138. Wilkens V, Sonntag S, Georg O. Robust spot-poled membrane hydrophones for measurement of large amplitude pressure waveforms generated by high intensity therapeutic ultrasonic transducers. J Acoust Soc Am. 2016;139(3):1319-32. doi: 10.1121/1.4944693. PubMed PMID: 27036269.
139. Zanelli CI, Howard SM. A robust hydrophone for HIFU metrology. In: Clement G, McDannold N, Hynynen K, editors. 5th International Symposium on Therapeutic Ultrasound; Boston, MA: Amer. Inst. Phys.; 2006. p. 618-22.
140. Parsons JE, Cain CA, Fowlkes JB. Cost-effective assembly of a basic fiber-optic hydrophone for measurement of high-amplitude therapeutic ultrasound fields. J Acoust Soc Am. 2006;119(3):1432-40. PubMed PMID: 16583887.
141. Haller J, Wilkens V, Jenderka KV, Koch C. Characterization of a fiber-optic displacement sensor for measurements in high-intensity focused ultrasound fields. J Acoust Soc Am. 2011;129(6):3676-81. doi: 10.1121/1.3583538. PubMed PMID: 21682392.
142. Zhou Y, Zhai L, Simmons R, Zhong P. Measurement of high intensity focused ultrasound fields by a fiber optic probe hydrophone. J Acoust Soc Am. 2006;120(2):676-85. PubMed PMID: 16938956; PMCID: PMC1994996.
143. Wear KA, Gammell PM, Maruvada S, Liu Y, Harris GR. Improved measurement of acoustic output using complex deconvolution of hydrophone sensitivity. IEEE Trans Ultrason

Ferroelectr Freq Control. 2014;61(1):62-75. doi: 10.1109/TUFFC.2014.6689776. PubMed PMID: 24402896.
144. Wilkens V, Koch C. Amplitude and phase calibration of hydrophones up to 70 MHz using broadband pulse excitation and an optical reference hydrophone. J Acoust Soc Am. 2004;115:2892-903.
145. Hurrell A. Are you getting 'phased' by the problem? J Phys Conf Series. 2004;1:57-62.
146. Eichstadt S, Wilkens V. Evaluation of uncertainty for regularized deconvolution: A case study in hydrophone measurements. J Acoust Soc Am. 2017;141(6):4155. doi: 10.1121/1.4983827. PubMed PMID: 28618819.
147. Liu Y, Wear KA, Harris GR. Variation of High-Intensity Therapeutic Ultrasound (HITU) Pressure Field Characterization: Effects of Hydrophone Choice, Nonlinearity, Spatial Averaging and Complex Deconvolution. Ultrasound Med Biol. 2017;43(10):2329-42. doi: 10.1016/j.ultrasmedbio.2017.06.012. PubMed PMID: 28735734; PMCID: PMC5639436.
148. Haller J, Jenderka KV, Durando G, Shaw A. A comparative evaluation of three hydrophones and a numerical model in high intensity focused ultrasound fields. J Acoust Soc Am. 2012;131(2):1121-30. doi: 10.1121/1.3675003. PubMed PMID: 22352487.
149. Canney MS, Bailey MR, Crum LA, Khokhlova VA, Sapozhnikov OA. Acoustic characterization of high intensity focused ultrasound fields: a combined measurement and modeling approach. J Acoust Soc Am. 2008;124(4):2406-20. doi: 10.1121/1.2967836. PubMed PMID: 19062878; PMCID: PMC2677345.
150. Rosnitskiy PB, Yuladashev PV, Vysokanov BA, Khokholva VA. Setting boundary conditions on the Khokholv-Zabolotskaya equation for modeling ultrasound fields generated by strongly focused transducers. Acoust Phys. 2016;62:153-62.
151. Kreider W, Yuldashev PV, Sapozhnikov OA, Farr N, Partanen A, Bailey MR, Khokhlova VA. Characterization of a multi-element clinical HIFU system using acoustic holography and nonlinear modeling. IEEE Trans Ultrason Ferroelectr Freq Control. 2013;60(8):1683-98. doi: 10.1109/TUFFC.2013.2750. PubMed PMID: 25004539; PMCID: PMC4130294.
152. Jing Y, Cannata J, Wang T. Experimental verification of transient nonlinear acoustical holography. J Acoust Soc Am. 2013;133(5):2533-40. doi: 10.1121/1.4796120. PubMed PMID: 23654362.
153. Sapozhnikov OA, Tsysar SA, Khokhlova VA, Kreider W. Acoustic holography as a metrological tool for characterizing medical ultrasound sources and fields. J Acoust Soc Am. 2015;138(3):1515-32. doi: 10.1121/1.4928396. PubMed PMID: 26428789; PMCID: PMC4575327.
154. Shimazaki Y, Harigane S, Yoshizawa S, Umemura S. Three-dimensional quantitative optical measurement of asymmetrically focused ultrasound pressure field. Jap J Appl Phys. 2012;51(07GF25-1).
155. Harigane S, Miyasaka R, Yoshizawa S, Umemura S. Optical phase contrast mapping of highly focused ultrasonic fields. Jap J Appl Phys. 2013;52:07HF.
156. Hariharan P, Myers MR, Robinson RA, Maruvada SH, Sliwa J, Banerjee RK. Characterization of high intensity focused ultrasound transducers using acoustic streaming. J Acoust Soc Am. 2008;123(3):1706-19. doi: 10.1121/1.2835662. PubMed PMID: 18345858.
157. Maruvada S, Liu Y, Pritchard WF, Herman BA, Harris GR. Comparative study of temperature measurements in ex vivo swine muscle and a tissue-mimicking material during high intensity focused ultrasound exposures. Phys Med Biol. 2012;57(1):1-19. doi: 10.1088/0031-9155/57/1/1. PubMed PMID: 22127191.
158. Holt RG, Roy RA. Measurements of bubble-enhanced heating from focused, MHz-frequency ultrasound in a tissue-mimicking material. Ultrasound Med Biol. 2001;27(10):1399-412. PubMed PMID: 11731053.
159. Lafon C, Zderic V, Noble ML, Yuen JC, Kaczkowski PJ, Sapozhnikov OA, Chavrier F, Crum LA, Vaezy S. Gel phantom for use in high-intensity focused ultrasound dosimetry.

Ultrasound Med Biol. 2005;31(10):1383-9. doi: 10.1016/j.ultrasmedbio.2005.06.004. PubMed PMID: 16223642.
160. Dunmire B, Kucewicz JC, Mitchell SB, Crum LA, Sekins KM. Characterizing an agar/gelatin phantom for image guided dosing and feedback control of high-intensity focused ultrasound. Ultrasound Med Biol. 2013;39(2):300-11. doi: 10.1016/j.ultrasmedbio.2012.09.016. PubMed PMID: 23245823.
161. Guntur SR, Choi MJ. An improved tissue-mimicking polyacrylamide hydrogel phantom for visualizing thermal lesions with high-intensity focused ultrasound. Ultrasound Med Biol. 2014;40(11):2680-91. doi: 10.1016/j.ultrasmedbio.2014.06.010. PubMed PMID: 25220272.
162. King RL, Liu Y, Maruvada S, Herman BA, Wear KA, Harris GR. Development and characterization of a tissue-mimicking material for high-intensity focused ultrasound. IEEE Trans Ultrason Ferroelectr Freq Control. 2011;58(7):1397-405. doi: 10.1109/TUFFC.2011.1959. PubMed PMID: 21768024.
163. Choi G, Park DH, Kang SH, Chung YG. Glioma mimicking a hypertensive intracerebral hemorrhage. J Korean Neurosurg Soc. 2013;54(2):125-7. doi: 10.3340/jkns.2013.54.2.125. PubMed PMID: 24175027; PMCID: PMC3809438.
164. Liu Y, Maruvada S, King RL, Herman BA, Wear KA. Development and characterization of a blood mimicking fluid for high intensity focused ultrasound. J Acoust Soc Am. 2008;124(3):1803-10. doi: 10.1121/1.2956469. PubMed PMID: 19045670.
165. Sun MK, Shieh J, Lo CW, Chen CS, Chen BT, Huang CW, Chen WS. Reusable tissue-mimicking hydrogel phantoms for focused ultrasound ablation. Ultrason Sonochem. 2015;23:399-405. doi: 10.1016/j.ultsonch.2014.10.008. PubMed PMID: 25453217.
166. Menikou G, Yiannakou M, Yiallouras C, Ioannides C, Damianou C. MRI-compatible bone phantom for evaluating ultrasonic thermal exposures. Ultrasonics. 2016;71:12-9. doi: 10.1016/j.ultras.2016.05.020. PubMed PMID: 27261569.
167. Menikou G, Damianou C. Acoustic and thermal characterization of agar based phantoms used for evaluating focused ultrasound exposures. J Ther Ultrasound. 2017;5:14. doi: 10.1186/s40349-017-0093-z. PubMed PMID: 28572977; PMCID: PMC5452295.
168. Farrer A, Odeen H, de Bever J, Coats B, Parker D, Payne A, Christensen D. Characterization and evaluation of tissue-mimicking gelatin phantoms for use with MRgFUS. Journal of Therapeutic Ultrasound. 2015;3(9).
169. Morris H, Rivens I, Shaw A, Haar GT. Investigation of the viscous heating artefact arising from the use of thermocouples in a focused ultrasound field. Phys Med Biol. 2008;53(17):4759-76. doi: 10.1088/0031-9155/53/17/020. PubMed PMID: 18701773.
170. Parker DL, Smith V, Sheldon P, Crooks LE, Fussell L. Temperature distribution measurements in two-dimensional NMR imaging. Med Phys. 1983;10(3):321-5. PubMed PMID: 6877179.
171. Clarke RL, ter Haar GR. Temperature rise recorded during lesion formation by high-intensity focused ultrasound. Ultrasound Med Biol. 1997;23(2):299-306. PubMed PMID: 9140186.
172. Kennedy JE, Wu F, ter Haar GR, Gleeson FV, Phillips RR, Middleton MR, Cranston D. High-intensity focused ultrasound for the treatment of liver tumours. Ultrasonics. 2004;42(1-9):931-5. PubMed PMID: 15047409.
173. Hynynen K. The threshold for thermally significant cavitation in dog's thigh muscle in vivo. Ultrasound in Med & Biol. 1991;17(2):157-69.
174. Maruvada S, Liu Y, Soneson JE, Herman BA, Harris GR. Comparison between experimental and computational methods for the acoustic and thermal characterization of therapeutic ultrasound fields. J Acoust Soc Am. 2015;137(4):1704-13. doi: 10.1121/1.4916280. PubMed PMID: 25920823.
175. Soneson JE. A user-friendly software package for HIFU simulation. American Institute of Physics2009. p. 165.

176. Huang J, Holt RG, Cleveland RO, Roy RA. Experimental validation of a tractable numerical model for focused ultrasound heating in flow-through tissue phantoms. J Acoust Soc Am. 2004;116(4 Pt 1):2451-8. PubMed PMID: 15532675.
177. Hariharan P, Myers MR, Banerjee RK. HIFU procedures at moderate intensities--effect of large blood vessels. Phys Med Biol. 2007;52(12):3493-513. PubMed PMID: 17664556.
178. Curra FP, Mourad PD, Khokhlova VA, Cleveland RO, Crum LA. Numerical simulations of heating patterns and tissue temperature response due to high-intensity focused ultrasound. IEEE Trans Ultrason Ferroelectr Freq Control. 2000;47(4):1077-89. doi: 10.1109/58.852092. PubMed PMID: 18238643.
179. Moros EG, Novak P, Straube WL, Kolluri P, Yablonskiy DA, Myerson RJ. Thermal contribution of compact bone to intervening tissue-like media exposed to planar ultrasound. Phys Med Biol. 2004;49(6):869-86. PubMed PMID: 15104313.
180. Nell DM, Myers MR. Thermal effects generated by high-intensity focused ultrasound beams at normal incidence to a bone surface. J Acoust Soc Am. 2010;127(1):549-59. doi: 10.1121/1.3257547. PubMed PMID: 20059000.
181. Myers MR. Transient temperature rise due to ultrasound absorption at a bone/soft-tissue interface. J Acoust Soc Am. 2004;115(6):2887-91. PubMed PMID: 15237812.